END

MICROCOPY RESOLUTION TEST CHART

NATIONAL BUREAU OF STANDARDS - 1963 - A
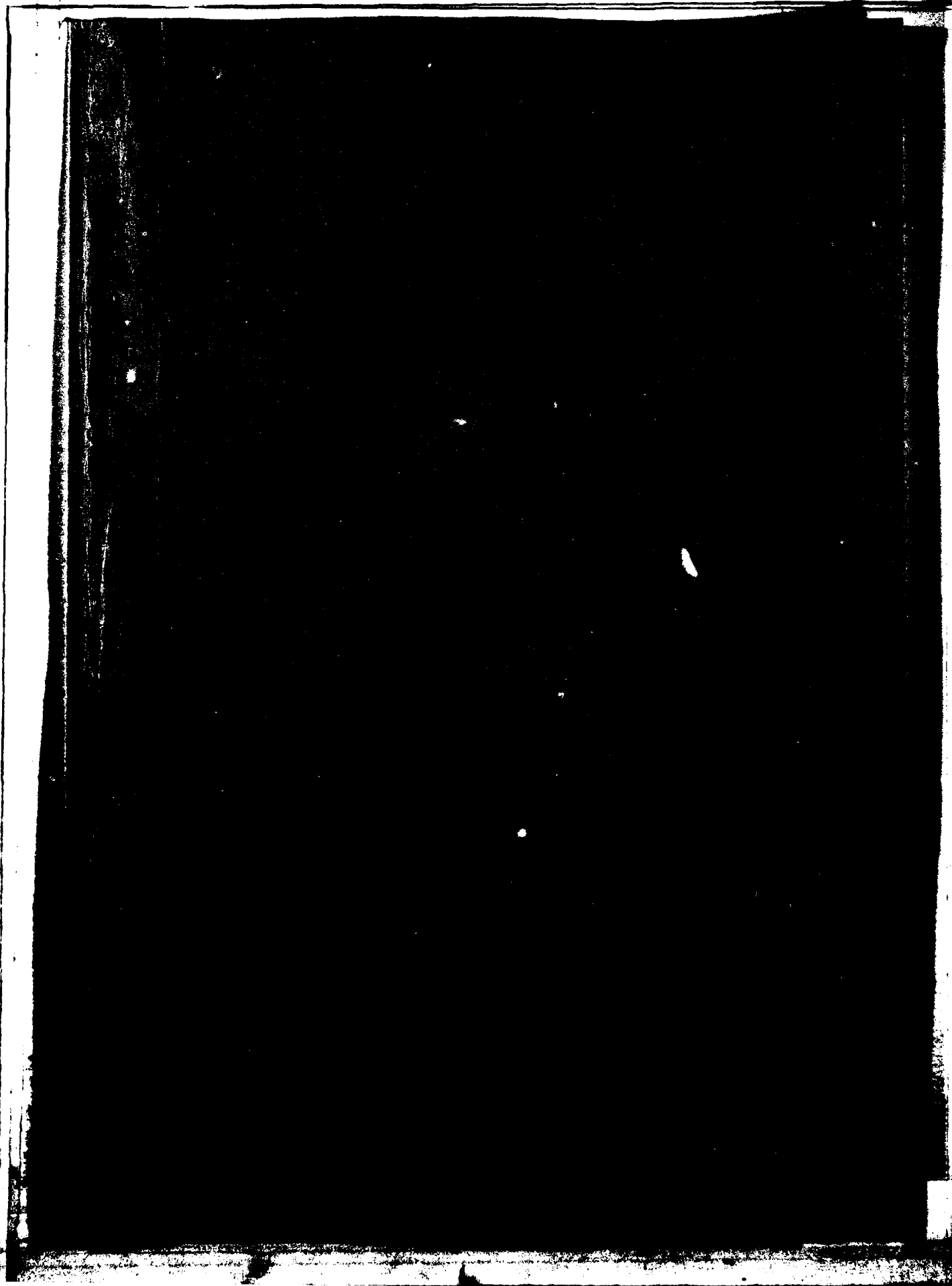
AD

HIGH TEMPERATURE FRICTION OF
CERAMIC AND CERMET COATINGS.

Final technical report
by

A. AZCARATE
J. BLOUET
JF. CRETEGNY
R. GRAS

JANUARY 1983

United States Army

EUROPEAN RESEARCH OFFICE OF THE U.S. Army

London England

CONTRACT NUMBER DAJA 37-81-C-0487

I. S. M. C. M.

REPORT DOCUMENTATION PAGE	READ INSTRUCTIONS BEFORE COMPLETING FORM

1. REPORT NUMBER	2. GOVT ACCESSION NO. AD-A135214	3. RECIPIENT'S CATALOG NUMBER

4. TITLE (and Subtitle)	5. TYPE OF REPORT & PERIOD COVERED
High Temperature Friction of Ceramic and Cermet Coatings	Final Technical Report May 82 – June 83
	6. PERFORMING ORG. REPORT NUMBER

7. AUTHOR(s)	8. CONTRACT OR GRANT NUMBER(s)
A. Azcarate, J. Blouet, JF Cretegny, R. Gras	DAJA37-81-C-0487

9. PERFORMING ORGANIZATION NAME AND ADDRESS	10. PROGRAM ELEMENT, PROJECT, TASK AREA & WORK UNIT NUMBERS
Laboratoire de Tribologie I.S.M.C.M., 3, rue Fernand Hainaut, 93407 Saint-Ouen, Cedex, France	6.11.02A IT161102BH57-04

11. CONTROLLING OFFICE NAME AND ADDRESS	12. REPORT DATE
USARDSG-UK Box 65 FPO NY 09510	January 1983
	13. NUMBER OF PAGES
	65

14. MONITORING AGENCY NAME & ADDRESS(If different from Controlling Office)	15. SECURITY CLASS. (of this report)
	Unclassified
	15a. DECLASSIFICATION/DOWNGRADING SCHEDULE

16. DISTRIBUTION STATEMENT (of this Report)

Approved for public release; distribution unlimited

17. DISTRIBUTION STATEMENT (of the abstract entered in Block 20, if different from Report)

18. SUPPLEMENTARY NOTES

19. KEY WORDS (Continue on reverse side if necessary and identify by block number)

Friction, Temperature, Carbide, Oxide, Coating, Ceramic, Cermic, Wear

20. ABSTRACT (Continue on reverse side if necessary and identify by block number)

The purpose of this study is the tribological analysis of coating materials containing basically ceramics and cermets, which can be sintered or sprayed. The materials studied were: – 69% TiC + 31% Ni – 80% CrₓCᵧ + 20% NiCr –25% WC + 5% Ni – 70% W/Cr – Cr₂O₃ – Al₂O₃ – x% Cr₂O₃ + (100-x% Al₂O₃. The tests were conducted by means of two high temperature tribometers, one working in a vacuum, and the other in air. The contact pressure was 1 N/mm² and the friction speed 5 m/mn. These conditions permitted us to disregard friction-induced temperature phenomena.

During each test, the normal load, the tangential load and the temperature were continuously recorded. After each test, other measurements were made, according to the requirements of the study, by using methods such as: - density measurements; wear coefficient measurements (using profilometry methods); hardness and microhardness; micrography; roughness; x-Rays; microscan; electronic microscope.

As for the friction of carbide-based coating; our study shows four phases, which depend on the temperature: - $T < 100°C$: influence of water films - $100°C$ $T < 400°C$: disappearance of water; metallic friction - $400°C$ $T < T_{ox}$: disappearance of metallic friction; appearance of large amounts of oxides that improve the friction - $T > T_{ox}$: catastrophic oxidation of the coating.

As for the friction of oxide-based coatings, our study shows the following: it was not possible to define a typical behaviour of the oxides, except that their friction was best between $400°C$ and T_{ox}. In all cases, the friction behaviour was shown to be related to the appearance of glazed films. A new chemical behaviour is proposed for Cr_2O_3, that explains its tribological behaviour. It was shown tht the behaviour of the coating of Al_2O_3 and Cr_2O_3 compounds was closely related to that of Cr_2O_3.

Finally, it should be noted that the carbide-based cermets are much more resistant to stress, within the temperature ranges studied, than the oxide-based coatings.

ABSTRACT

The purpose of this study is the tribological analysis of coating materials containing basically ceramics and cermets, which can be sintered or sprayed. The materials studied were :

- 69% TiC + 31% Ni

- 80% Cr_7C_3 + 20% NiCr

- 25% WC + 5% Ni - 70% W/Cr

- Cr_2O_3

- Al_2O_3

- x% Cr_2O_3 + (100-x)% Al_2O_3

The tests were conducted by means of two high temperature tribometers, one working in a vacuum, and the other in air. The contact pressure was 1 N/mm^2 and the friction speed 5 m/mn. These conditions permitted us to disregard friction-induced temperature phenomena.

During each test, the normal load, the tangential load and the temperature were continuously recorded. After each test, other measurements were made, according to the requirements of the study, by using methods such as :

- density measurements
- wear coefficient measurements (using profilometry methods)
- hardness and microhardness
- micrography
- roughness
- X-Rays
- microscan
- electronic microscope

As for the friction of carbide-based coating, our study shows four phases, which depend on the temperature :

- $T < 100°C$: influence of water films.

- $100°C < T < 400°C$: disappearance of water ; metallic friction.

- $400°C < T < T_{ox}$: disappearance of metallic friction ; appearance of large amounts of oxides that improve the friction.

- $T > T_{ox}$: catastrophic oxidation of the coating.

As for the friction of oxide-based coatings, our study shows the following : it was not possible to define a typical behaviour of the oxides, except that their friction was best between 400°C and T_{ox}. In all cases, the friction behaviour was shown to be related to the appearance of glazed films. A new chemical behaviour is proposed for Cr_2O_3, that explains its tribological behaviour. It was shown that the behaviour of the coating of Al_2O_3 and Cr_2O_3 compounds was closely related to that of Cr_2O_3.

Finally, it should be noted that the carbide-based cermets are much more resistant to stress, within the temperature ranges studied, than the oxide-based coatings.

- CONTENTS -

- ILLUSTRATIONS -

Figure 1 : Thermal cracking during friction.

Figure 2 : Cracking of the coatings due to increase of the ambient temperature.

Figure 3 : Shape of the samples.

Figure 4 : Evolution of the coefficient of friction of TiC-Ni sliding against itself in air, versus time.

Figure 5 : Evolution of the coefficient of friction of Cr_7C_3-NiCr sliding against itself in air, versus time.

Figure 6 : Evolution of the coefficient of friction of carbide based coatings, sliding against themselves in air, versus temperature.

Figure 7 : Evolution of the coefficient of friction of carbide based coatings sliding against themselves in a vacuum of 10^{-6}mm Hg, versus temperature.

Figure 8 : Measures of microhardness in TiC-Ni coatings.

Figure 9 : Measures of microhardness in Cr_7C_3-NiCr coatings.

Figure 10 : Curve of the atomic concentration of the elements at one point of the surface, versus ionic erosion time for TiC-Ni after testing in air at 700°C (glazed area).

Figure 11 : Same as above (non glazed area).

Figure 12 : Curve of the atomic concentration of the elements of one point of the surface, versus ionic erosion time : TiC-Ni after testing in a vacuum at 700°C (glazed area).

Figure 13 : Same as above (non glazed area).

Figure 14 : Curve of the atomic concentration of the elements of one point of the surface, versus ionic erosion time : Cr_7C_3-NiCr after testing in air at 900°C - glazed area.

Figure 15 : Same as above (non glazed area).

Figure 16 : Effect of the Ni binder on the sliding friction of TiC-Ni, sliding against itself in a vacuum.

Figure 17 : Evolution of the coefficient of friction of Cr_2O_3 sliding against itself in air, versus time.

Figure 18 : Evolution of the coefficient of friction of Cr_2O_3 sliding against itself in air, versus temperature.

Figure 19 : Evolution of the coefficient of friction of Cr_2O_3 sliding against itself in air, versus the apparent contact pressure.

Figure 20 : Cumulative wear, measured after each grade of pressure.

Figure 21 : Evolution of the coefficient of friction of alumina Al_2O_3 sliding against itself in air, versus temperature.

Figure 22 : Evolution of the coefficient of friction of Al_2O_3 sliding against itself in air, versus apparent pressure.

Figure 22 bis : Evolution of the coefficient of friction of alumina sliding against chromium oxide in air, versus temperature.

Figure 23 : Variation of the coefficient of friction of alumina sliding against chromium oxide in air, versus time.

- TABLES -

Table 1 : Composition of the tested cermets.

Table 2 : Composition of the substrates.

Table 3 : Characteristics of the testing materials.

Table 4 : Roughness parameters Ra and Rt of the surfaces of
TiC-Ni after tests at 20, 250, 700 and 820°C.

Table 5 : Roughness parameters Ra and Rt of the surfaces of
Cr_7C_3-NiCr after tests at 400, 700 and 900°C.

Table 6 : Roughness parameters Ra and Rt of the surfaces of
Cr_2O_3 after tests at 20, 225, 550, 700 and 850°C.

Table 7 : Cr/Al and Al/Cr ratios measured respectively on
Al_2O_3 and Cr_2O_3 after tests at 400 and 900°C.

Table 8 : Variation of the roughness parameters Ra and Rt of
Al_2O_3 and Cr_2O_3, versus test temperature.

I - INTRODUCTION

There are two principal origins for the idea of causing friction between oxides and carbides, which are related to two not very recent observations.

For one thing, it was realized that, with dry sliding of these metals, oxidation could be a factor of noticeable improvement in the conditions of friction.

In addition, we know that the mechanical properties of metals decline rapidly with increases in temperature, while the so-called refractory materials are only subject to this defect at much higher temperatures.

Among these refractory materials, we have oxides and carbides that are relatively easy to obtain, and that also have quite remarkable mechanical properties at high temperature.

High temperature work is necessitated by progress in technology (aeronautics and aerospace science) as well as by improvements in efficiency (automobile motors and turbines, for example) involving significant energy savings.

It has become indispensable for us to understand in full the friction mechanisms of refractory materials, as well as to define the parameters influencing this friction.

II - BIBLIOGRAPHY

2.1 - Ceramic and metallo-ceramic materials :

Ceramics are metallic or non metallic inorganic composites, generally very hard, fragile and refractory with ionic or covalent bonding.

In the high temperature applications which are of interest to us, two types of ceramics are used :

- intermetallic binary composites such as carbides, nitrides and silicides
- metallic oxides.

They have remarkable properties at high temperatures, but their fragility at low temperatures and their susceptibility to thermic and mechanical shocks have so far limited their applications.

The need for modern technologies to obtain mechanisms that are functional at high temperatures, and recent progress in obtaining suitable materials, permit us to anticipate the use of these materials, that are the only ones capable of resolving certain problems such as high temperature friction.

Metallo-ceramic materials represent a compromise between the toughness and refractoriness of ceramics, and the conductivity and impact resistance of metals. Among materials of this type, we took particular interest in cermets, composed of a continuous ceramic network impregnated with metal. Both contribute to the solidity of the structure, and to its behaviour during high temperature tribological applications.

2.2 - Sliding friction and wear :

2.2.1 : Interactions between the surfaces and causes of friction :

All surfaces are rough at the microscopic scale. Contact between surfaces therefore occurs at the level of their asperities. Under such

conditions, the real contact area is only a fraction of the nominal contact area.

BOWDEN and TABOR [1], believe that during sliding very strong adhesive connections appear that must be sheared. This adhesive force could therefore be the primary cause of friction (Fad). Ploughing forces have to be added when there is a big difference between the hardnesses of the materials (Fpl). So, the friction force F can be written :

$$F = Fad + Fpl$$

Despite criticisms, this conception of friction is often accepted because it permits the explanation of many tribological situations, particularly at high temperatures : in most cases, it seems possible to neglect ploughing with respect to adhesion.

2.2.2 : Wear mechanisms :

Generally, four fundamental wear mechanisms are considered :

- adhesion : the formation and shearing of connections between the asperities of the surfaces. It is enhanced by cleanness of the surfaces, plastic deformations, chemical affinity of the materials, and elevation of the temperature. It is often characterized by transfer phenomena of the materials during friction.

- abrasion and shearing : wear as a consequence of the displacement of matter, caused by hard particles or protuberances.

- fatigue : a result of cyclic stresses affecting the superficical layers of the contacting bodies. It induces and spreads cracks under the surfaces. These cyclic stresses can be either mechanical or thermal.

- tribochemical reactions : the formation of new products due to chemical interactions between the sliding bodies or (and) between them and the environment.

In most cases, these mechanisms are combined in a more or less complex way to gradually induce the failure of the sliding bodies. In order to limit the activity of these mechanisms, it is important for the materials

to have certain properties [2]:

- considerable hardness with a fine grain and a homogeneous structure.
- sufficient toughness with respect to all the constraints imposed on the system.
- correct properties at elevated temperatures (retention of hardness at high temperatures).
- high thermodynamic stability.
- high resistance of all grain boundaries
- low tendancy to adhere.

Friction tests on metal samples in oxidizing atmosphere at elevated temperatures [3], have shown a reduction of the friction coefficient. This is related to the formation of an oxide layer thick enough to protect the metal crystals and only permit adhesion at higher levels of deformation, and higher temperatures.

2.3 - Tribological behaviour of ceramic and cermet materials :

2.3.1 : Behaviour of monocrystals :

The observations made by many authors about monocrystals lead, generally, to the following points :

2.3.1.1 : Anisotropy :

The friction and wear behaviour of most ceramic monocrystals is anisotropic, and varies with cristallographic plane and orientation.

2.3.1.2 : Adhesion :

In the contact area, very strong adhesive connections can appear. However, the specific characteristics of ionic or covalent bonding in ceramics suggest that such connections are much less likely than in metals. Adhesive forces between two ceramic bodies, or between a ceramic body and a metal, are influenced by crystallographic orientations.

2.3.1.3 : Plasticity :

It has often been observed that, in spite of their reputation for

brittleness, ceramic materials behave plastically at the contact scale. It has been noted that, if these epidermic deformations can occur at room temperature, massive deformations require very high temperatures.

2.3.1.4 : Adsorption :

The presence of adsorbed films influences the mechanical properties, and, therefore, the sliding properties, of ceramic materials. Some adsorbed products can be tensioactive and induce large variations in the behaviour of the materials during friction. Adsorption of polar liquids can significantly influence the mobility of dislocations and the hardness of the materials close to the surfaces. They increase the capacity of the surfaces for plastic deformation, by inhibiting brittle cracking during friction. The negative effect of desorption is often shown by testing in a high vacuum.

2.3.2 : Polycrystalline ceramic materials and cermets :

2.3.2.1 : Introduction :

Most of the observations made on monocrystals are valid for polycrystalline ceramic applications as well. However, the anisotropic behaviour of monocrystals is not observed in materials whose surfaces are composed of a mosaïc of grains with no particular orientation.

Ceramic materials generally have a low dilation coefficient and low thermal conductivity, but a high melting point and a high degree of hardness and resistance to oxidization. However, their brittleness at low temperatures is a serious limitation for many applications. Compared to ceramics, cermets have the following advantages : higher tenacity and ductility and therefore better shock resistance. On the other hand, as the metal percentage increases, hardness and refractarity decrease, while the adhesivity and wear rate increase.

Most of the phenomena that influence the tribological behaviour of ceramics and cermets depend to a great extent on the temperature : adhesion, adsorption, real contact area, and so on.

2.3.2.2 : Adhesion :

Adhesion is caused by molecular forces of attraction which arise

between two surfaces, independent of any lateral force, and which can remain when these forces have disappeared. It is still not known how adhesion can be evaluated precisely, though the theory of BOWDEN and TABOR 1 , improved by RABINOWICZ [4] has clarified a great deal : it takes into account the adhesion work W_{ad} (defined by DUPRE in 1869), which depends on materials, temperature, adsorbed films, etc.

The main phenomena influencing the adhesion of ceramics and cermets are the following :

2.3.2.2.1 : Crystallographic orientation :

The adhesion of ceramics is greatly influenced by the crystallographic orientation of the surfaces : a small relative disorientation of the atomic lattice on both sides of the interface considerably reduces the forces of attraction. Polycrystals will therefore have a much lower tendancy to adhere than well-oriented monocrystals.

2.3.2.2.2 : Mutual solubility :

The theory developed for metals and adhesion led to the establishment of strong links between the mutual solubility of pairs of materials and their adhesion. It is thought that soluble pairs adhere well (Fe - Al for instance), and that non-soluble pairs have weak adhesive interactions (Cr - Ag for instance). However, some exceptions limit the applications of this theory.

With ceramics, studies concerning mutual solid solubility [5] tend to indicate that the correlation is quite low between friction and wear on the one hand, and the concept of solubility on the other.

This may be due to the formation, observed by many authors, of interfacial films which condition the friction and wear behaviour of ceramics.

2.3.2.2.3 : Chemical reactivity of the surfaces :

BUCKLEY [6] indicates that electronic interactions between superficial atomic layers have a greater influence on adhesion than does mutual solubility : the greater the chemical reactivity between the surfaces, the higher the force of adhesion.

2.3.2.2.4 : Effect of temperature :

Adhesion can become very important if the critical temperature of

adhesion is reached [1,7] . This temperature can be 0.3 to 0.65 times the melting temperature Tm, depending on the materials (metals, oxides). This critical temperature decreases as the applied load increases.

This phenomenon is attributed to the combination of antagonistic effects : on the one hand, increases in temperature and duration of contact cause increases in the real area of contact ; on the other hand, variations in the temperature and breaking speed cause variations in the mechanical stresses of the bindings.

Variation of the real contact area occurs through several steps. These are mainly :

  elastoplastic deformation during loading
- increase of the real area of contact, due to two phenomena :

        . the flow of the asperities
        . the sintering of the asperities (even without load)

These two phenomena are caused by the action of physicochemical phenomena that are generally thermoactivated.

So, it was stated that the real area of contact varies like an Arrhenius law :

$$Ar = Ao . \exp (- Q_A/R.T) . t_A^{1/n}$$

with :   R = perfect gas constant

        Q_A = activation energy of the preponderant physical phenomenon in the temperature field studied

        t_A = duration of contact

        n = an index between 2 and 8, depending on the physical mechanisms

2.3.2.3 : Chemical transformations :

During sliding, chemical transformations can occur close to the interface, creating many compounds. When they are present, these transformations determine friction and wear. If some corrosions are harmful, and even catastrophic, from the friction and wear point of view, other reactions can have beneficial effects, and sometimes be used as lubrication. We classified the chemical transformations undergone by the materials during friction into two groups :

        - transformations caused by reactions with the atmosphere
        - transformations caused by reactions between solids

2.3.2.3.1 : Reactions with the atmosphere :

Here we will only consider oxidation - reduction phenomena.

Without friction, the parameters that influence the growth of the oxide layer are, mainly, temperature, the partial pressure of oxygen, and the diffusion speed of anions and cations. Generally, the observed laws of oxide layer growth are linear or parabolic.

With friction, the growth of the oxide layer depends on the rate of growth by oxidation versus the rate of wear : generally, the thicker the oxide layer, the slower its growth. Two types of destruction can be predicted :

- if the superficial layer is brittle, it is removed in scales as soon as its thickness reaches a critical value : the wear rate is high.

- if the superficial layer is ductile, the shearing will occur in the film, and the wear rate will be low.

An elevation of the oxidizing temperature during friction can induce an increase in the thickness of the oxide film and therefore a decrease in the oxidizing rate, followed by a decrease in the wear rate [8].

2.3.2.3.2 : Reactions between solids :

The reactions that can occur between solids are classified into two groups :
- additive reactions : $A + B \quad AB$
- exchange reactions : $AB + CD \quad AD + BC$

Depending on the nature of the primary oxides, the additive reactions will produce either a solid solution or a double oxide :

- solid solution : $AO + BO \quad (AB)O$
- double oxide   : $AO + BO \quad ABO_2$

These behaviours depend very much on the crystalline structure of the oxides, as well as on the nature of the primary metals and the basicity or acidity of their oxides.

The exchange reactions that occur during oxidation are essentially

of the following type :

A + BO   AO + B   , like, for instance,

Fe + NiO   FeO + Ni
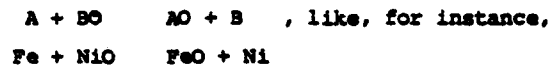
These reactions are characterized by the appearance of two new compounds.

2.3.2.4 : Cracking :

In a simple traction test, two types of rupture were identified : ductile and brittle. The elementary distinction between them is related to the presence or absence of plastic deformations before rupture.

Ductile rupture is the result of the formation and growth of cupules, while brittle rupture may correspond to an intergranular decohesion, or, more generally, to an intergranular cleavage.

The concept of brittleness implies a relationship with time as well : the brittle or ductile behaviour of a material depends, to a great extent, on the speed of the increase in stress and strain. It is pointless to discuss whether a given material is "ductile" or " brittle" ; we can only discuss, its ductile or brittle behaviour under given test conditions. A crack with a brittle type evolution is a rupture by separation. Division of the material due to shearing is excluded by definition. Consequently, brittle rupture always occurs perpendicularly to the principal tractive stress of the moment.

The cracking of materials can have many origins such as mechanical overloads or variations in temperature. Among the mechanical cracks, we can observe several situations :

2.3.2.4.1 : Static case :

In the static case, Hertz hypotheses are used : the radius 'a' of the contact area between a sphere of radius 'r', and a plane, follows the law :

$$a^3 = \frac{1}{K} \ W \ r$$

where W is the applied load, and K a constant that depends on the materials (if a number 1 is given to the sphere and a number 2 to the plane, K is given by :

$$\frac{1}{K} = \frac{3\pi}{4} \ \ \frac{1 - \mu_2}{E_1} + \frac{1 - \mu_2}{E_2}$$

However, a linear relationship has sometimes been observed between the critical load inducing cracks, and the radius of the sphere : Wcrit. = A . r, while Hertz predicts a proportionnality between W and r^2.

2.3.2.4.2 : Dynamic case :

This is the case of shock. The hertzian theory can still be used as long as the duration of contact is long compared to the duration of the propagation of elastic waves in the highly stressed zones close to the contact area.

2.3.2.4.3 : Cracks due to friction :

When there is friction of a hemispherical part on a plane, the friction-induced tangential load modifies the stress near the contact [9]. For brittle materials, the appearance of tensile stresses is extremely important. Their intensity increases with the coefficient of friction μ . The radial stress σy stops being tensile in the front part of the sphere when μ reaches 0.079.

2.3.2.4.4 : Delamination :

Delamination corresponds to the development, through fatigue mechanisms, of cracks parallel to the sliding plane. We suggest that the steps leading up to this phenomenon are [10, 11]:

- plastic deformation of the superficial layers and creation of dislocations
- interaction among the dislocations, and between the dislocations and other obstacles (inclusions)
- coalescence of the dislocations and formation of empty spaces and cracks
- propagation of the cracks

2.3.2.4.5 : Effects of temperature :

Thermally induced fissuration is due to differential dilations between some parts of the bodies. It can develop at uniform temperature (anisotropy of the coefficients of dilation), or appear because of thermal gradients (thermal anisotropy).

During cycles of heating and cooling, thermal fatigue phenomena can be observed.

Friction is an important cause of variations in temperature. This temperature can reach the melting point of one of the materials, especially at the level of the contacting asperities. Their low calorific capacity leads to the sudden appearance of high temperature : this is the flash temperature.

From studies performed by Jaeger [12], it is possible to conclude that temperatures are influenced more by speed than by load, and that the temperature decreases rapidly in the interior of the part. This implies that, on the one hand, the thermal stresses due to friction are extremely superficial, and, on the other hand, that a small change in the thermal properties of a thin superficial layer can induce large variations in the superficial temperature.

The shape of the thermally induced cracks has the general appearance shown in fig 1 :
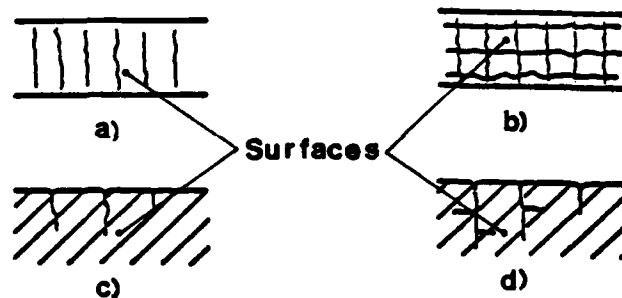
figure 1 : Thermal cracking during friction :

        a) and b) : surface appearance
        c) and d) : cross - section

2.3.2.5 : The glazes :

During friction of ceramics and cermets, one can sometimes observe the formation of an extremely thin superficial layer, with a polished and dense appearance. Many authors believe that this layer is responsible for the improvement of friction and wear in oxidizing atmosphere. These "glazes" were observed on many materials (steels, various compounds, ceramics, etc).

2.3.2.5.1 : Nature of the glazed layer :

This glazed layer, the thickness of which is around 1 micrometer, was frequently thought to be formed by oxides from the elements of the sliding pair (when the atmosphere allows oxidization), for metallic surfaces as well as for carbide or nitride ceramics. It was frequently reported that these oxides could produce eutectic compounds that "lubricate" the surface more efficiently than the "parent" oxides. The presence of graphite was sometimes observed in these oxide layers.

Opinions concerning the structure of the glazed layer are divided as to whether this structure is amorphous or crystalline. The formation of a vitreous layer can be explained by severe chill effects [13], or by the presence of materials with pasty melting as for certain oxides such as : SiO_2, B_2O_3, etc [14, 15, 16] .

Crystallinity and thickness can, generally, be related. When a coating is set in very thin layers, it is possible for it not to crystallize (thickness 2 m). For instance, amorphous layers can be obtained by physical deposition in vapor phase with : Al_2O_3, Cr_2O_3, etc. _ [17, 18, 19].

But it has also been stated that glazes can be crystallized, composed of sub-microscopic crystals (100 to 500 A° in diameter) of compacted oxides. RIGNEY, GLAESER and HIRTH [20, 21] have developped a theory according to which repeated plastic deformations accumulate in a very thin superficial layer. This highly deformed layer would have a microcrystalline structure with a high degree of preferred orientation. BOWDEN and TABOR indicate that viscous sliding of the grain joints can occur under shearing stresses, with a viscosity coefficient that is exponentially related to temperature.

2.3.2.5.2 : Formation mechanisms of glazed layers :

Four kinds of investigations were suggested concerning these mechanisms :

- mechanical action : this is action that results in glazes, through deformation and removal of matter (lapping). First, a truncation of the highest asperities occurs, followed by a filling in of the hollows by the resulting wear debris.

- thermal action : thermal phenomena resulting from friction contributes to
  the formation of the glazes through welding and softening. Vitreous layers
  can thus be obtained through a quick elevation of the temperature up to
  the point where welding of the material occurs, followed by a cooling rate
  that exceeds a certain value which depends on the material : too low a rate
  would allow recrystallization of the superficial layer.
  Another consequence of thermal action is the possibility of induction of
  an adiabatic plastification [22, 23] : during high speed tests, the sliding
  would be essentially adiabatic because of the very quick heating of a
  superficial layer that allows shearing at the interface, and explains the
  variations of friction with speed. In addition, it was observed that the
  insulating power of the ceramics is favorable to this action.

- compaction of the wear debris : the debris can contribute to the flattening
  of the surfaces by filling in the surface hollows. But their real contribution
  seems to be much more important, resulting in the formation of a crystalline
  film made of tiny compacted debris. Oxidization seems to be a contributing
  factor in this process : the glazes appear more quickly at high temperature,
  when the surfaces oxidize more easily. The wear rate is then low, because
  the wear debris, composed of tiny oxide particles, can be reinserted in the
  glaze during friction.

- plastification by adsorption : adsorption by the surfaces of tensioactive
  products would also be one of the causes of the appearance of glazes [24].
  This influence of the environment can, however, be decreased by an increase
  in temperature, lowering the adsorption of the active component.

2.3.3 : Specific behaviours of the coatings :

The most important parameters concerning the coatings are the
following :

2.3.3.1 : Thickness of the coatings :

The thinness of the coating allows the substrate to bear the applied
load. But the coating is more heat resistant and harder than the substrate.

Therefore, the flow of the substrate, because of the load or the temperature, can induce splits in the coating, or the shearing of the substrate/coating interface. Acceleration of the destructive processes of the film results. The thickness influences the capacity of the film to follow the deformations of the substrate, or to withstand thermal shocks. When the coating is thick enough, it bears the whole applied load and, from a tribological point of view, it behaves like a massive material.

2.3.3.2 : Adhesion on the substrate, compatibility :

The choice of the substrate is closely related to the nature of the coating : it is necessary for the substrate and the coating to have reasonable chemical compatibility, to avoid excessive chemical interaction during deposition or functioning. Excessive interdiffusion can change the nature of the coating itself, or permit the constituants of the substrate one wanted to mask, appear on the surface. On the other hand, too weak an interaction may have harmful consequences, for it limits the creation of metallurgical connections between coating and substrate.

But the adhesion of the coating on the substrate may be due to more than chemical phenomena. Indeed, purely mechanical considerations may be of some importance, like the simple hooking of the coating to the asperities of the substrate : here the notion of roughness of the substrate appears, which can be of great importance.

There can be still other influences of the substrate : chemical instability can induce distensions, distorsions or cracks.

The coefficients of dilation of the substrate and the coating are obviously of great importance : they have to be as close as possible, in order to minimize the shearing stresses at the interfaces during variations in temperature. Intermediate layers are sometimes introduced between the substrate and the coating, in order to permit better adhesion of the coating, or in order to decrease the stresses due to variations in temperature (with layers having an intermediate coefficient of dilation between that of the substrate and that of the coating).

During possible splitting of the coating, due to thermal stresses, it is the adhesion between the substrate and the coating that will determine the mode of splitting, because of their different coefficients of dilation.

Good adhesion will induce splits in the coating, while weaker adhesion will induce splits in the interface, as shown in fig. 2

High adherence   Low adherence
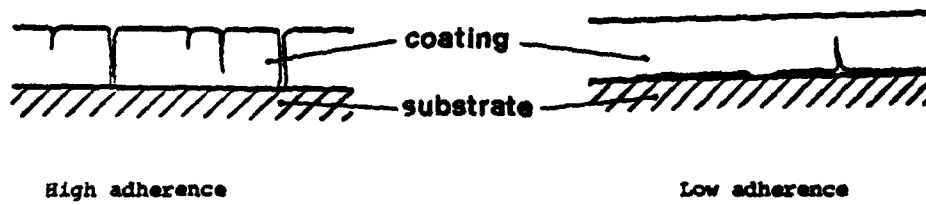
figure 2 : Cracking of the coatings due to increase of the
           ambient temperature.

III - EXPERIMENTAL STUDY

31 : Test conditions

311 : Materials :

The study deals with the behaviour of ceramic and cermet materials under conditions of dry sliding friction. The tests were conducted in air, and in a vacuum when it was necessary to check the influence of the atmosphere. We analysed friction between 20 and 1000°C.

Two types of materials were used :

- Metallic carbide based cermets
- Oxide based ceramics

These materials were used as coatings.

3-111- Metallic carbide based cermets

We began our study with the metallic carbide based cermets indicated in table 1 :

Coating	Substrate	Thickness (μm)	Roughness Ra μm	Process of Manufacture	Hardness Uv 0,01 Pa	
TiC-NI (69) (31)	XC 35	300	grinding 0.55	P	850	high dispersion
Cr_7C_3-NiCr (80) (20)	Inconel	50	lapping 0.1	G.D.	1020	
WC-Ni- W/Cr (25) (5) (70)	Inconel 600	-	lapping 0.14	G.D.	1560	

Table 1

P - Plasma deposition

G D - Gun deposition

The table 2 gives the composition of the substrates :

Composition of the materials used as substrates	
Steel XC 35	0,32-0,38 C, 0,50-0,80 Mn, 0,10-0,40 Si, < 0,035 P, < 0,035 S, Fe Complement
Inconel 600	16 Cr, 7 Fe, < 1 Mn, < 0,5 Cu, < 0,5 Si, < 0,15 C, < 0,015 S, Ni Complement

Table 2

3-112- <u>Oxide based ceramics</u>

The various materials used and their characteristics are given in table 3 :

Coating	Substrate	Thickness (m)	Roughness Ra m	Process of Manufacture	Hardness Uv 0,01 Pa
Cr_2O_3	Inconel 600	150	grinding 0,21	P.	1100
		50	lapping 0,12	P.	
Al_2O_3	Inconel 600	150	grinding 0,20	P.	1080
		50	lapping 0,15	P.	
x% Cr_2O_3 +(100-x%)Al_2O_3	Inconel 600	150	lapping	P.	--

Table 3

3.1.2.- <u>Test parts</u>

    3.1.2.1- Shape of the parts

The shape of the parts is given in fig. 3.
They are flat rings with parallel faces on which the sliding occurs, giving a plane/plane contact.

$\phi 6.5 {}^{-0.05}_{-0}$

40

$30 {}^{-0.1}_{-0}$

$1,5 \times 45°$

$6,75 {}^{\pm 0.05}$

$1,5 \times 45°$

$13,5 {}^{+0.1}_{+0}$

- a -

Counterpart   Slider

- b -
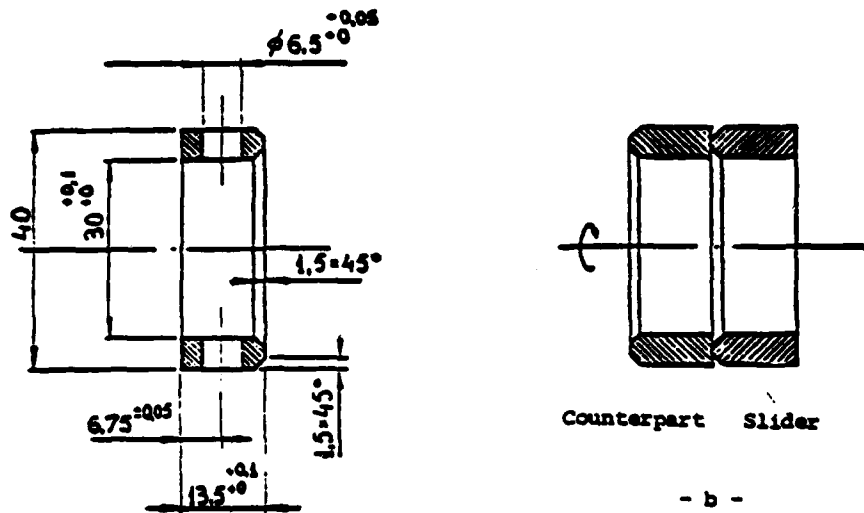
figure 3 : Shape of the samples

    a - Cross section

    b - Position of the samples during testing :

        - moving part   : counterpart

        - stationary part : slider

3-122- <u>Manufacture of the test samples</u>

Rings made of the two materials composing the substrates were machined by turning, after which the bases were ground. This grinding was followed by sanding. Then the coating was applied by plasma deposition or gun deposition.

The surfaces were finished by grinding or lapping.

In the case of nickel oxide, the coating was obtained by thermal oxidation of pure nickel.

Random samples of each type of material were taken for reference and analyzed by scanning electron microscope, X Rays and microhardness measurements.

3.1.3 : Apparatus :

Two test machines were used for the study, one functionning in oxidizing atmosphere, the other in a vacuum. Both used the same samples.

3.1.3.1 : High temperature friction apparatus in air

This friction apparatus, called FHTO, was designed to carry out high temperature friction tests in air. Its main characteristics are the following :

- Load Range :
- Speed Range :
- Temperature Range :

The friction coefficient can be continuously recorded. The temperature is measured at three points : one in the furnace, two in the samples.

The load is applied by means of dead weights for loads under 1000 N and by means of pneumatic jack for heavier loads. In the latter case it can be continuously recorded.

The rotating speed of the driving shaft can continuously vary in the whole field of speed of the apparatus.

3.1.3.2 : High temperature friction apparatus in a vacuum

The apparatus was designed to carry out tests in a vacuum. Its main characteristics are the following :

- Load Range   : 0 to 500 N
- Speed Range   : 0 to 1.75 m/s . (0 to 950 rpm)
- Temperature Range : 20 to 1500°C

- Vacuum Range : 1.3×10^{-4} Pa

The load is applied by means of dead weights.

3.1.3.3 : Measurement of friction coefficient

Both high temperature friction apparatus used the same principle :
one of the samples rotates (the moving piece) ; the other test piece (the
slider) is submitted to frictional torque and bonded to the measurement
system. The frictional torque, C_F, at the level of the surfaces is expressed
by :

$$C_F = \int_0^{2\pi} \int_{R_1}^{R_2} \mu \cdot p_a \cdot r^2 \quad dr \, d$$

$$= 2/3 . \pi . \mu . p_a . (R_2^3 - R_1^3)$$

with $\qquad \mu$ = friction coefficient

p_a = nominal contact pressure

If W is the applied load, we can write :

$$C_F = \frac{2}{3} \mu . W . \frac{R_1^2 + R_1 R_2 + R_2^2}{R_1 + R_2}$$

We measure this torque by means of a strength transducer situated at a
distance "a" from the rotating axle (a = 200 mm for the air apparatus,
a = 160 mm for the apparatus in a vacuum).
The value of the friction force is :

$$Fa = \frac{2}{3} \mu . W . \frac{R_1^2 + R_1 R_2 + R_2^2}{R_1 + R_2}$$
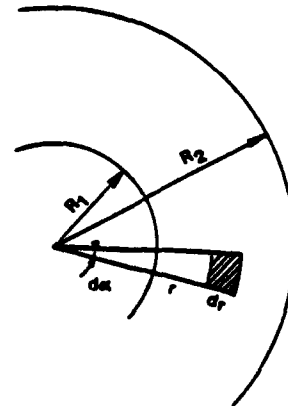
and therefore

$$= \frac{3}{2} \cdot a \cdot \frac{R_1 + R_2}{(R_1^2 + R_1R_2 + R_2^2)} \cdot \left(\frac{F}{W} \right)$$

3.1.4 : Experimental method

3.1.4.1 : Sample preparation :

Before each test, the samples were cleaned in two steps by immersion in an ultra-sonic bath. The first soaking in a grease removing bath of trichlorethylene was followed by a second bath in sulfuric ether. The samples were completely dried by a hot air stream.

3.1.4.2 : Conducting tests :

Before and after each test, the measuring system was balanced to eliminate errors resulting from a possible drift of their components.

We performed two types of tests called :

- continuous tests (or normal)
- sequential tests

3.1.4.2.1 : Continuous tests

In this type of test, load, speed and temperature are fixed and we record the evolution of the friction coefficient over time.

3.1.4.2.2 : Sequential tests

In this type of test, only two of the three variables are fixed : load, speed and temperature : the third varies in steps (generally 3 minutes each).

Most of the sequential tests were performed varying the temperature, for it was the main parameter. So we performed tests at various temperatures : 20 - 200, 400, 550, 700 - 800, 900 and 1000°C. Between each test the samples

were separated until the desired temperature was reached in order to avoid sticking.

The main reason for such sequential tests is to save material and time. We will demonstrate later on that such a method is quite acceptable.

3.1.4.2.3 : Experimental conditions :

Most of the tests were done under the following conditions of speed and load :

- contact pressure : 1 N/mm^2
- speed : 5 m/mn (45.5 tr/mn)

Under these conditions, and with a maximum coefficient of friction $\mu = 1$, the power per surface unit that has to be turned into heat is 0.083 W/mm^2. This low value permits us to disregard variations in temperature induced by friction.

Reductions in mass were only considered after the low temperature tests (under 250°C). After higher temperature tests, no significant measure was obtainable because of the development of thermal splits and subsequent destruction of the coatings, due to different coefficients of dilatation for the coating and substrate.

The majority of the tests were done in an oxidizing atmosphere. Some tests were done in a vacuum, simply to complement our investigations into the nature of the friction of our materials (no adsorbed films, no oxygen).

3.2 : Tests results :

3.2.1 : Friction of the carbide based cermet coatings :

The cermets tested in this study are the following :

- Titanium carbide with Nickel die
- Chromium carbide with Nickel-chromium die
- Tungsten carbide with Nickel and W-Cr carbides

3.2.1.1 : Friction tests :

The results of the friction tests of identical materials sliding against each other in air are shown in figures 4, 5, 6 and 7.
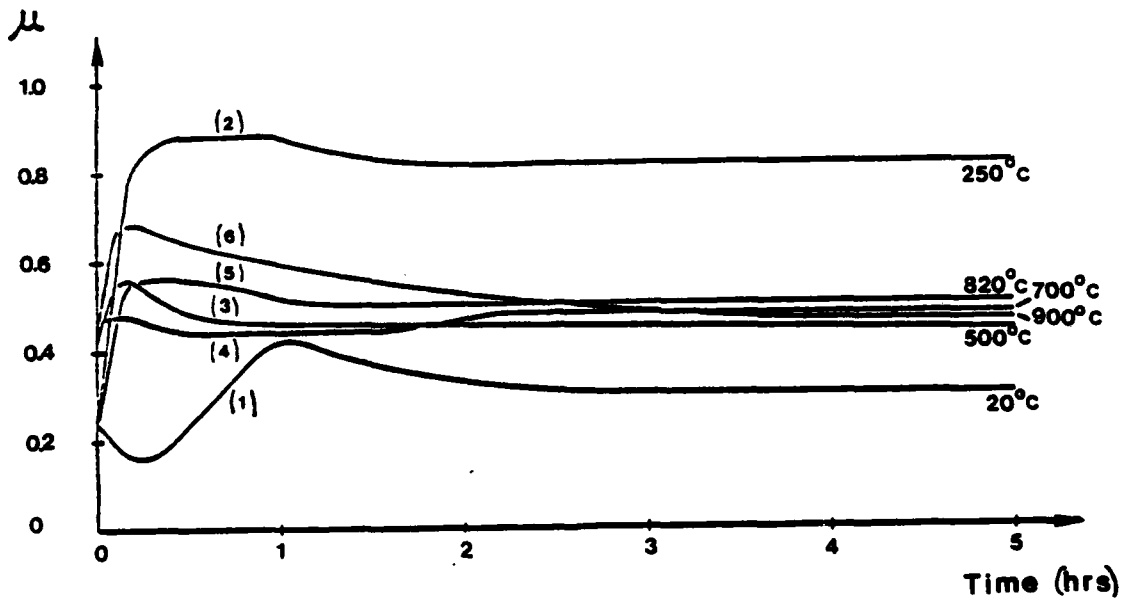
figure 4 : Variation of the coefficient of friction of TiC-Ni sliding against itself in air, versus time (1 N/mm^2, 5 m/mn, 20 - 250 - 500 - 700 - 820 - 950°C)

( ) in parentheses : test number
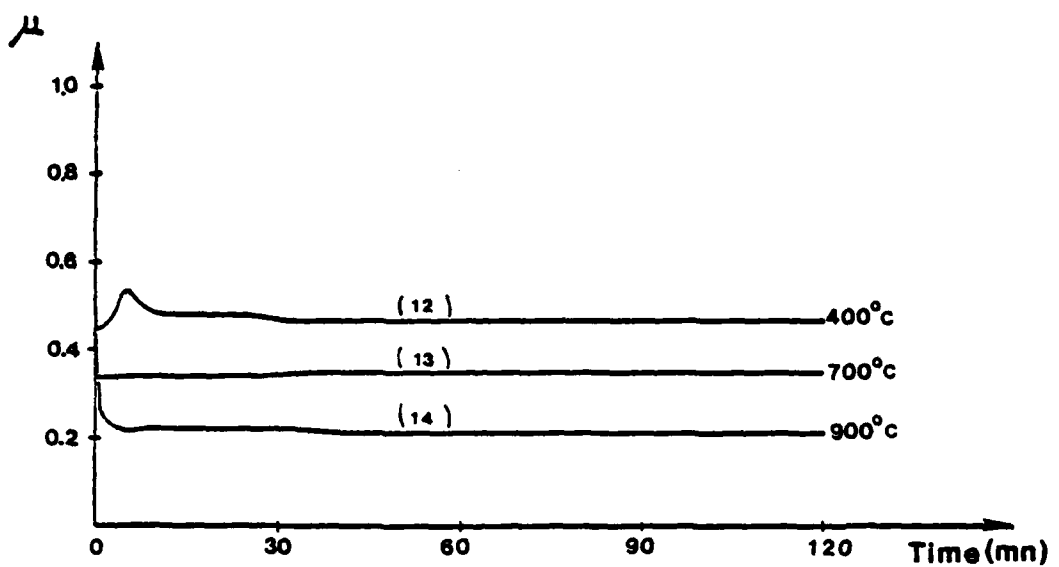
figure 5 : Variation of the coefficient of friction of Cr_7C_3-NiCr sliding against itself in air, versus time (1 N/mm^2, 5m/mn, 400 - 700 - 900°C)

( ) in parentheses : test number
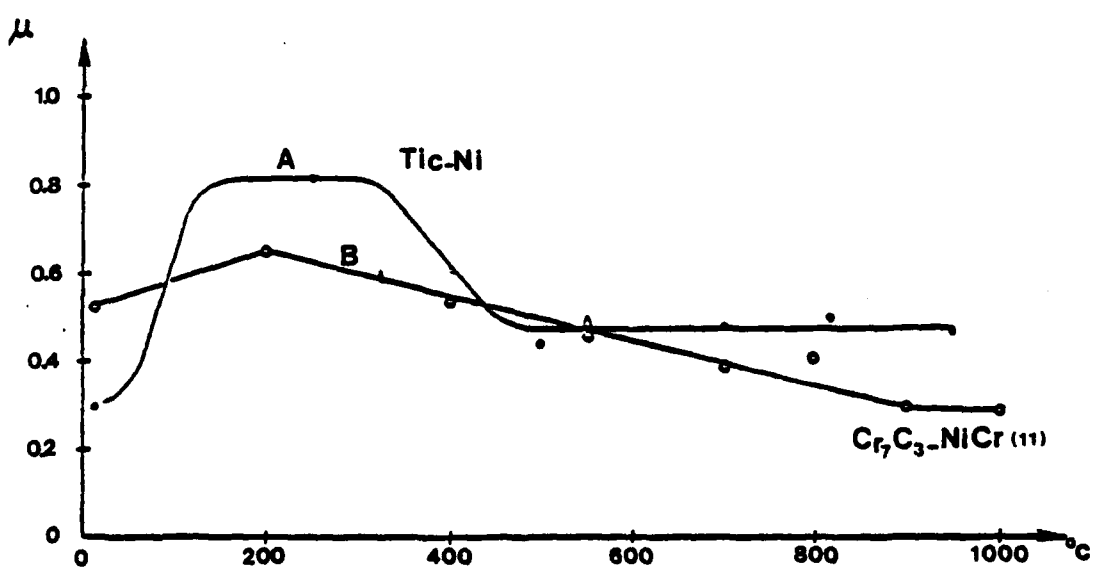
figure 6 : Evolution of the coefficient of friction of carbide based coatings sliding against themselves in air, versus temperature (1 N/mm^2, 5 m/mn)

( ) in parentheses : test number
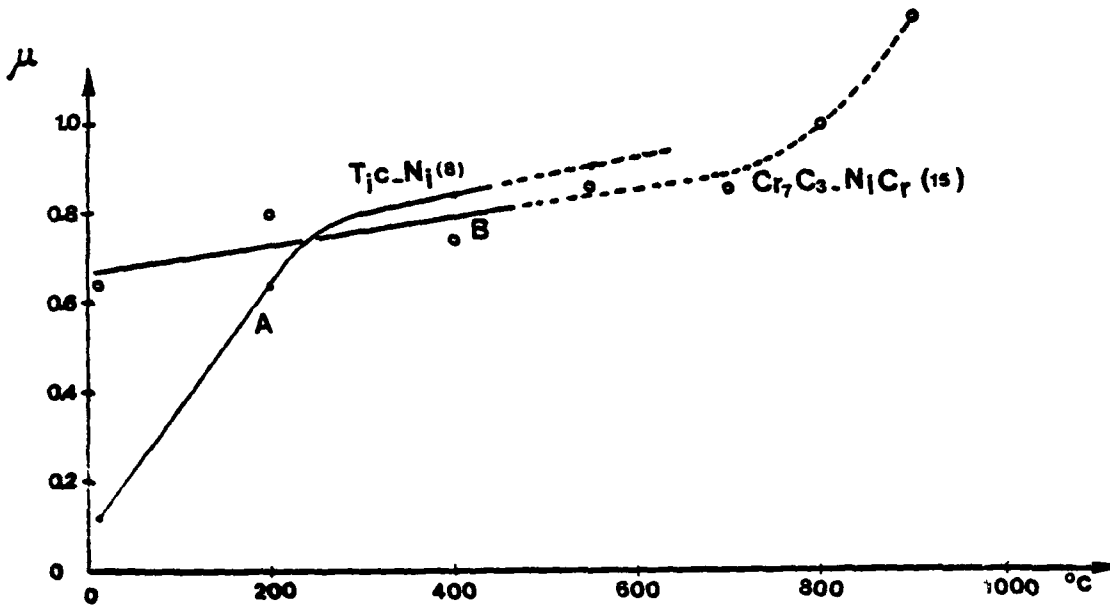
figure 7 : Evolution of the coefficient of friction of carbide based coatings
sliding against themselves in a vacuum of 10^{-6} mm Hg, versus
temperature. (1 N/mm^2, 5 m/mn)
( ) in parentheses : test number

In the case of titanium carbide with nickel die, continuous tests have
been carried out at the following temperatures :
20, 250, 500, 700, 820, 950°C.
These tests were used to draw the A curve of figure 6 (coefficient of friction
versus temperature).
For Chromium Carbide - Nickel Chromium, the process was different :
the shape of the curve was determined rapidly by a sequential test. Some normal
tests permitted us to check this shape and therefore confirm the value of our
tests (fig. 6)
The results of the friction tests of identical materials sliding
against themselves in a vacuum are shown in figure 7. They were determined thanks
to sequential tests. At high temperatures, the test was interrupted after 10 to

30s of friction (instead of 3 mn), because of the high level of chattering
reached and the resulting danger for the vacuum apparatus. At temperatures
between about 100 and 300°C, an increase in the pressure was observed (up to
1. 3×10^{-3} Pa), because of desorption phenomena as well as the release of
oxygen occluded in the coatings during manufacture.

3.2.1.2 : Analyses of the samples :

The couples of samples were systematically analysed after testing
by different means, such as electronic microscope, microscan, X Ray diffraction,
microhardness measurements.

3.2.1.2.1 : Electronic microscopy and microanalyses :

An extremely detailed analysis of the surfaces and of the wear
fragments was done by electronic microscopy, and thus typical characteristics
of some physicochemical transformations were obtained.

It was possible to detect the nature of the constituent elements of
the surface and to determine their proportions by means of microanalyses on
the surfaces and in depth, and to relate them to the temperature of the tests.
In the case of titanium carbide - nickel, the ratio Ni/Ti was observed.

In the case of chromium carbide - nickel we were interested in the
Ni/Cr ratio. In both cases, we noticed a decrease of these ratios with the
increase of the temperature. It reaches a minimum around 700°C, corresponding
to the appearance of glazes.

3.2.1.2.2 : X-ray diffraction :

X-ray analysis of the surfaces permitted identification of the
superficial layers of the samples as well as determination of the proportions
of these compounds.

So, in the case of TiC-Ni, we observed the appearance of 3 compounds
above 500°C : NiO, Ni TiO_3, and TiO_2. As the temperature increases, the
proportion of TiO_2 increases as well, and becomes largest on the surface
above 950°C. This phenomenon was not observed in a vacuum. We also observed

that $NiTiO_3$ is essentially found in the wear debris, for ultrasonic cleaning of the surfaces divides the proportion of this compound by four.

In the case of Chromium Carbide - Nickel Chromium, we could observe above 400°C, the appearance of oxides on the surfaces (in lower quantities than with TiC-Ni). In addition, we never detected Nickel oxide : various authors write that the oxidation of NiCr should produce nickel oxide and chromium oxide. Only the latter was found, which suggests that it was the result of the oxidation of chromium carbide. This is an extremely interesting observation, because of the freeing of carbon induced by this reaction, as we will see in the following pages.

3.2.1.2.3 : Microgeometry :

Tables 4 and 5 show roughness parameters Ra and Rt of the TiC-Ni and Cr_7C_3 - NiCr coatings. At low temperatures, the surfaces are damaged. When the temperature increases, the surface roughness decreases as a consequence of the appearance of glazes. The roughness parameters of these glazes are in the same range as those of the best polishings. In the case of TiC-Ni, elevating the temperature too much increases oxidation and produces splits and cracks that lead to the destruction of the surfaces.

3.2.1.2.4 : Microhardness :

MEYER introduced the following empirical law :

$$W = a \, d^n$$

in which W is the load, d the diagonal of the Vickers imprint, "a" a constant and "n" another constant called Meyer's index. The drawing of our results in logarithmic coordinates has given figures 8 and 9, each point being the mean of at least six measures.

Testing Temperature (°C)	Before test	20	250	700	820
Ra (m)	0.575	0.717	0.320	0.010	0.504
Rt (m)	7.190	6.744	2.827	0.079	5.963

Table 4 : Roughness parameters Ra and Rt of the surfaces of TiC-Ni after continuous type tests at 20, 250, 700 and 820°C.

Testing Temperature (°C)	Before test	400	700	900
Ra (m)	0.096	0.262	0.101	0.034
Rt (m)	2.194	3.178	2.392	0.576

Table 5 : Roughness parameters Ra and Rt of the surfaces of Cr_7C_3-NiCr after continuous type tests at 400, 700 and 900°C.

H_V Load (g)	Before Sliding	After testing at 250°C	After testing at 900°C
15	1207 (4.8)	1634 (4.1)	1314 (4.6)
25	1132 (6.4)	1532 (5.5)	1187 (6.25)
50	1071 (9.3)	1314 (8.4)	1049 (9.4)
100	846 (14.8)	1048 (13.3)	960 (13.9)
200	720 (22.7)	882 (20.5)	865 (20.7)
300	675 (28.7)	829 (25.9)	829 (25.9)

- H_V in daN/mm^2
- (—) average value of the diagonal in μm

TiC_NI / TiC_NI

Before Sliding
After Testing at 250°C
After Testing at 700°C

$n_{=}1.59$
$n_{=}1.73$
$n_{=}159$
$n_{=}1.82$
$n_{=}1.68$
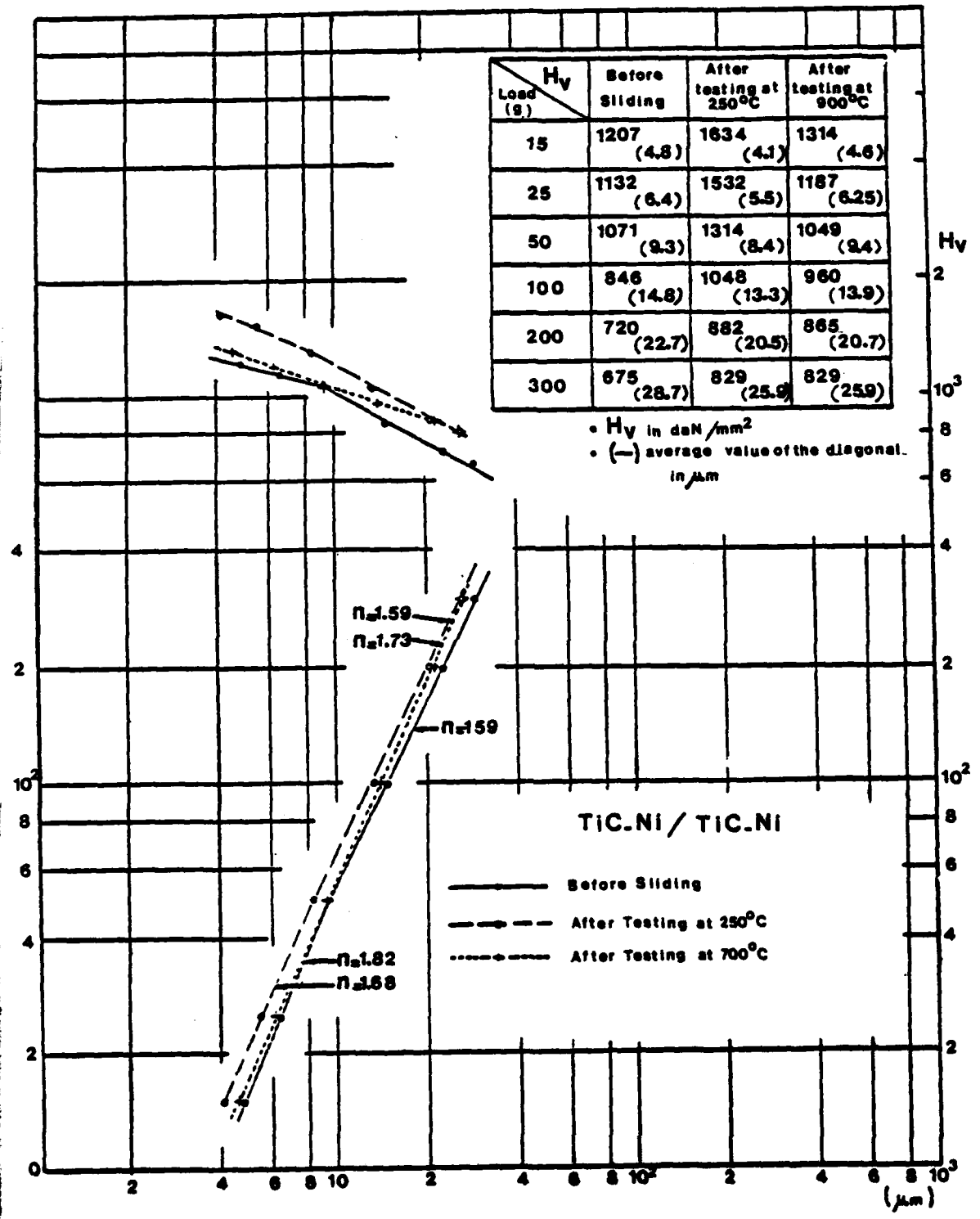
figure 8 : Measures of microhardness in TiC-Ni coatings.

Above : Log Hv = f(Log d) ; below : Log W

$Cr_7C_3 - N_iCr / Cr_7C_3 - N_iCr$

1. —•— Before Sliding
2. —•— After testing of 120′ at 400°C
3. —•— After testing of 120′ at 900°C

H_v

$n \approx 1.87$ $n = 1.67$
$n \approx 1.82$
$n \approx 1.56$
$n \approx 1.69$
$n \approx 1.84$

H_v / Load (g)	Before Sliding	After testing at 250°C	After testing at 900°C
15	2031 (3.7)	1926 (3.8)	—
25	1714 (5.2)	1854 (5)	2757 (4.1)
50	1485 (7.9)	1485 (7.9)	2336 (6.3)
100	1150 (12.7)	1309 (11.9)	2143 (9.3)
200	995 (19.3)	1225 (17.4)	1670 (14.9)
300	919 (24.6)	1170 (21.8)	1625 (18.5)

- H_v in daN/mm²
- ( ) average value of the diagonal in μm

$d(\mu m)$
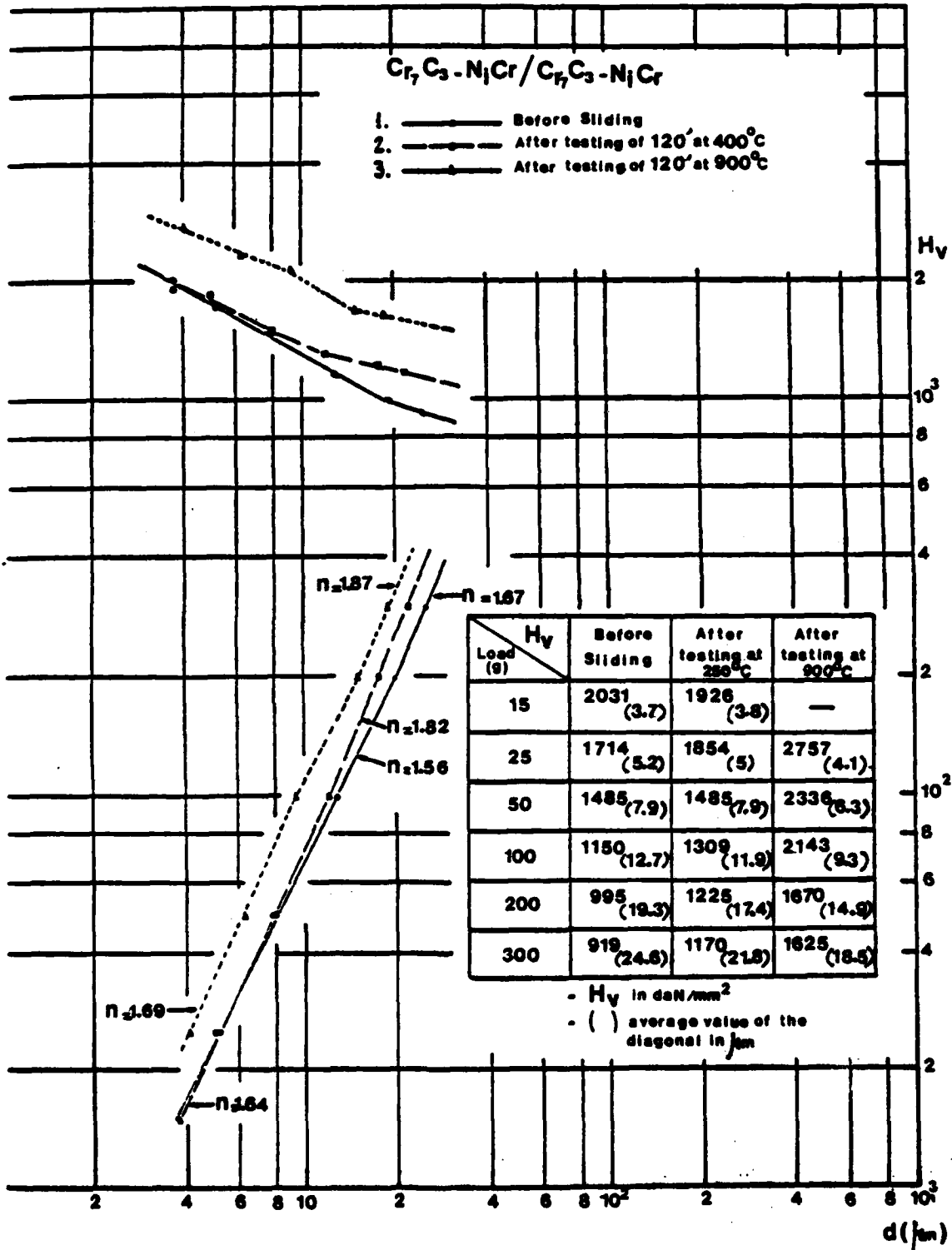
figure 9 : Measures of microhardness in Cr_7C_3 - NiCr coatings.
Above, $\text{Log } H_v = f(\text{Log } d)$; below, $\text{Log } W = f(\text{Log } d)$ (H_v = microhardness, d = diagonal ; W = load ; n = slope)

Figure 8 shows the results concerning TiC-Ni. Before testing and with small loads ($<$ 50g), we observed that the index (n = 1.82) was similar to the one of nickel (n = 1.85). This indicates that a thin layer of Ni was spread on the surface during machining. At higher loads ($>$ 50g), we again find the hard and brittle characteristics of the coating, because the carbide supports the load : a low n (around 1.3 to 1.7) corresponds to a hard and brittle material ; a high n (around 1.8 to 2.1) corresponds to a soft and ductile material. After the 250°C test, a translation of the curve is observed, the slope of which remains the same at elevated loads. At low loads, a decrease of the slope is observed because of the elimination of the surface layer as well as the work-hardening of the material. After the 700°C test, the appearance of an oxide-based glazed layer is observed. Its hardness is lower than that of TiC, but higher than that of nickel. The Meyer index therefore has its value between those of these two materials : n = 1.73.

In the case of Cr_7C_3-NiCr (fig. 9), the same principles were applied. Before testing, the material is brittle. After a 900°C test, a oxyde based glazed layer appears, mainly composed of Cr_2O_3, which is much harder than the carbide phase.

3.2.1.3 : Discussion :

The results of our friction tests in air show that :

- the coefficient of friction passes through a transition period before becoming constant. The higher the ambient temperature (in given limits) the shorter and the lower the transition period.

- the behaviour of the material is influenced by temperature, even after stabilisation. As the temperature increases, the curves describing the evolution of the coefficient of friction of the three materials tested keep the same shape. Our analyses clearly show two friction behaviours : the first appears below

400°C and its main characteristics are the presence of the
binder and the absence of oxides on the surface. The second
appears above 400°C and is characterized by a decrease in
the amont of binder on the surface and the formation of
significant quantities of oxides.

However, a more precise analysis, based on the evolution of the coefficient
of friction, permits a division in two of each of these phases.

3.2.1.3.1 : First phase of the friction : T < 100°C

For the study of this phase, we only used TiC-Ni. The coefficient
of friction is quite low, but the friction is very unstable. This low
coefficient of friction may be due to the presence of adsorbed films, among
which we can cite water vapour, which could induce the following phenomena :

- reduction of the chemical interaction between the contacting
  surfaces.

- evacuation of the thermal energy produced by the friction.

Electronic microscopy of the surfaces after testing shows typical
characteristics of adhesion and abrasion : this is due to the metallic-ceramic
structure of the coating. Abrasive wear is produced by the presence of hard
debris caused by the progressive intergranular fracture of the carbide grains.
Adhesion is produced by the presence of nickel, which increases the wear
resistance of the cermet. Indeed, the rate of wear produced by plastic
deformation is smaller than the rate of wear produced by fracture. In addition,
the nickel fills the pores of the surfaces, improves the bonding of the
carbide grains and stops, by plastic deformation, the intergranular progression
of fractures which would lead to a high rate of wear. This is confirmed by
observation of the Ni/Ti ratio, which is about 0.61 after testing when it
was 0.52 before : we thus observe a spread of the nickel on the surface.

3.2.1.3.2 : Second phase of friction : 100°C < T < 400°C

Between 100°C and 400°C, we have performed normal type tests on samples coated with TiC-Ni (250°) and Cr_7C_3-NiCr (400°C).

In this field of temperature, a quick deterioration of the coefficient of friction is observed as a consequence of the disappearance of adsorbed films. At the same time, a significant increase in wear is observed : we have calculated that the normal load capable of inducing fractures in TiC at 250°C is ten times lower than at 20°C. The carbide grains are therefore more easily worn by fracture than during the first phase.

In the case of TiC-Ni, the Ni/Ti ratio increases very little : it is equal to 0.54 after testing while it was equal to 0.52 before. The nickel sprayed on the surfaces is immediately abraded.

In the case of Cr_7C_3-NiCr, we proceeded to testing at the limit of the phase (400°C). The worn surfaces showed many abrasive scratches, as well as adhesive damage. There too, we observed an increase in the ratio Ni/Cr from 0.10 to 0.13.

3.2.1.3.3 : Third phase of friction : 400°C < T < T_{ox}

The T_{ox} temperature depends on the material used : it is the temperature above which we observed catastrophic oxidization. It is about 800°C for TiC-Ni and 1000°C for Cr_7C_3-NiCr. During this third phase, we observed the formation of large amounts of oxides which induce improvement of friction and decrease in wear.

Up to about 100°C below T_{ox}, we observed very low wear with production of a fine powder composed of particles of oxides from the coatings. Then, when the temperature approaches T_{ox}, we obtain a regular and soft friction at the beginning of the test as well as the formation of a glazed surface, the wear of which is negligible. The thickness of this glaze is about 10^{-6}m (1 µm).

Microhardness measurements show differences in the nature of the glazed layers of TiC-Ni and Cr_7C_3-NiCr. With the first material, we observed that the hardness and the Meyers index are located between those of the material before testing and those of the work-hardened material. With the second, the glazes are much harder than the substrate, but the Meyers indexes are similar.

The extremely low roughness of the glazes is shown in tables 4 and 5. These layers are compounds of oxides and carbon, which gradually comes from the oxidization of the carbide. It then diffuses across the oxide layer and reaches the sliding interface where it contributes to the development of the glazes. The composition of the glazes was determined by Auger electron microscopy (figures 10 to 15).
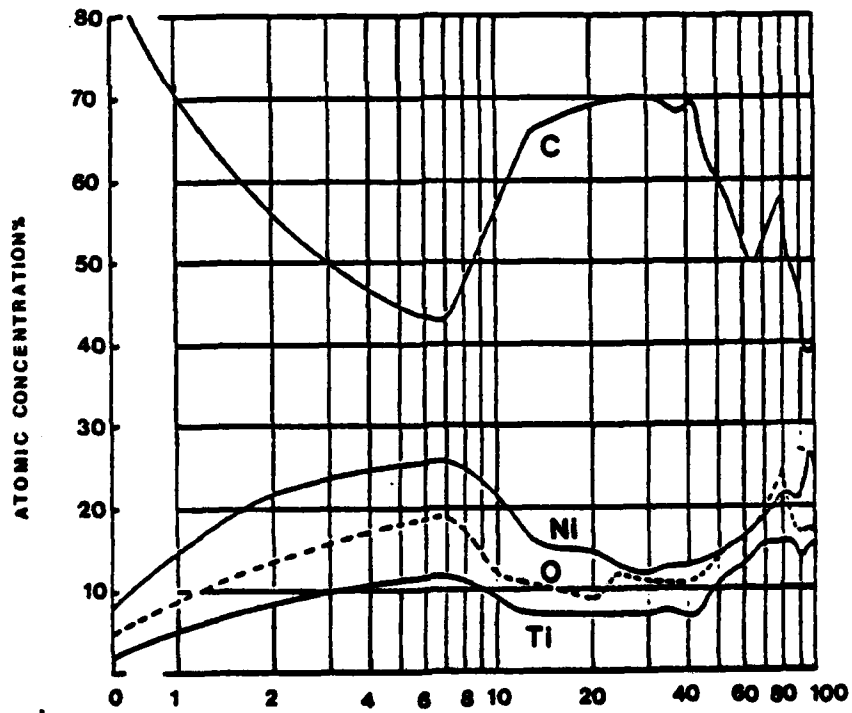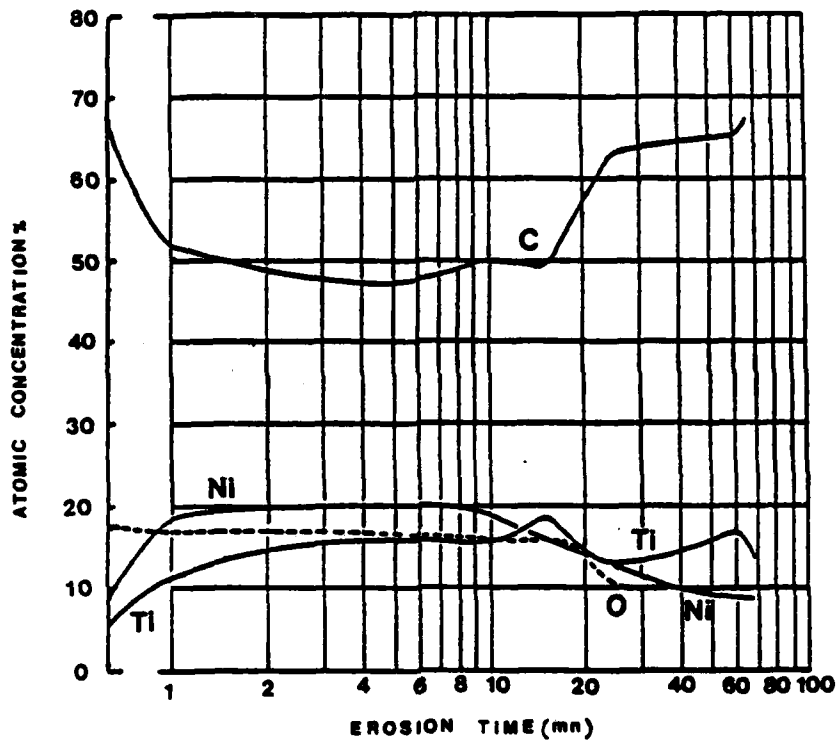
figure 10 : Curve of the atomic concentration of the elements at one point of
the surface, versus ionic erosion time, for TiC-Ni after testing
in air at 700°C (glazed area)

figure 11 : As above. Non-glazed area

figure 12 : Curve of the atomic concentration of the elements of one point of
the surface, versus ionic erosion time : TiC-Ni after testing in
a vacuum at 700°C - glazed area
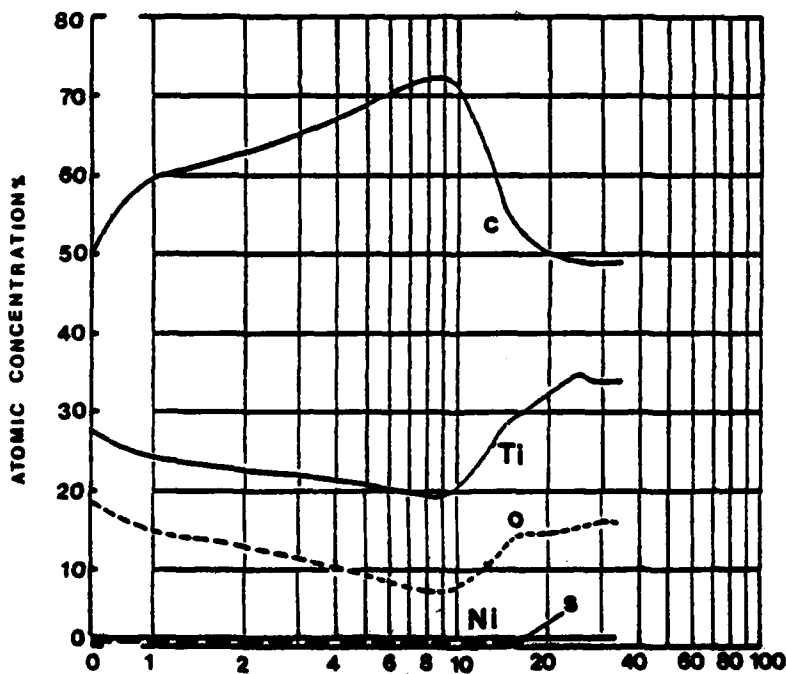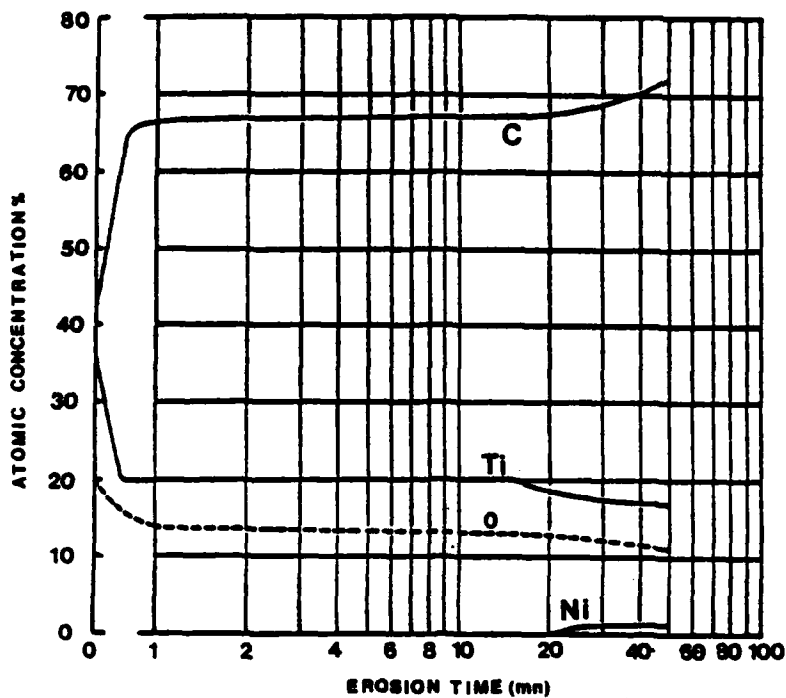
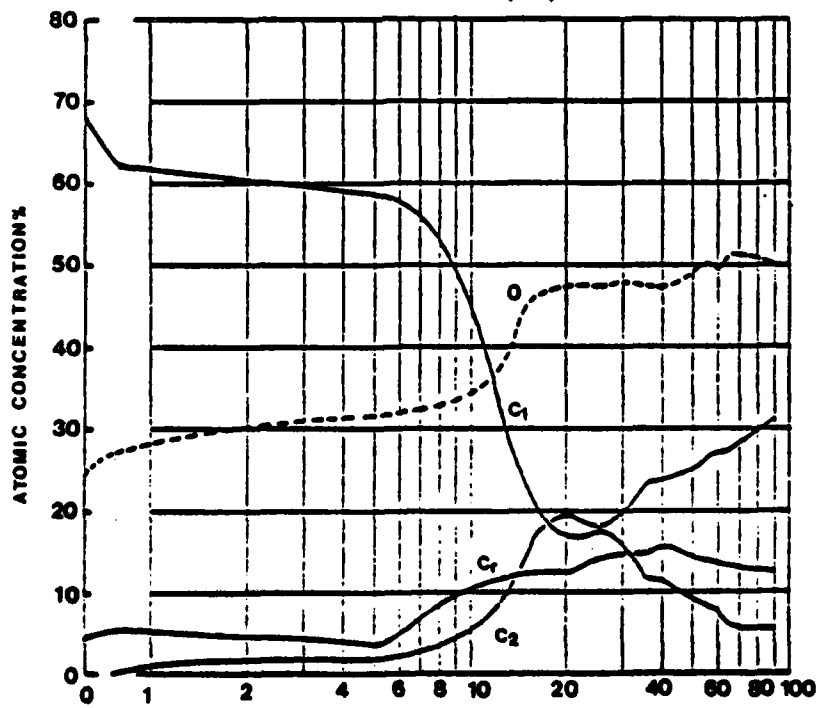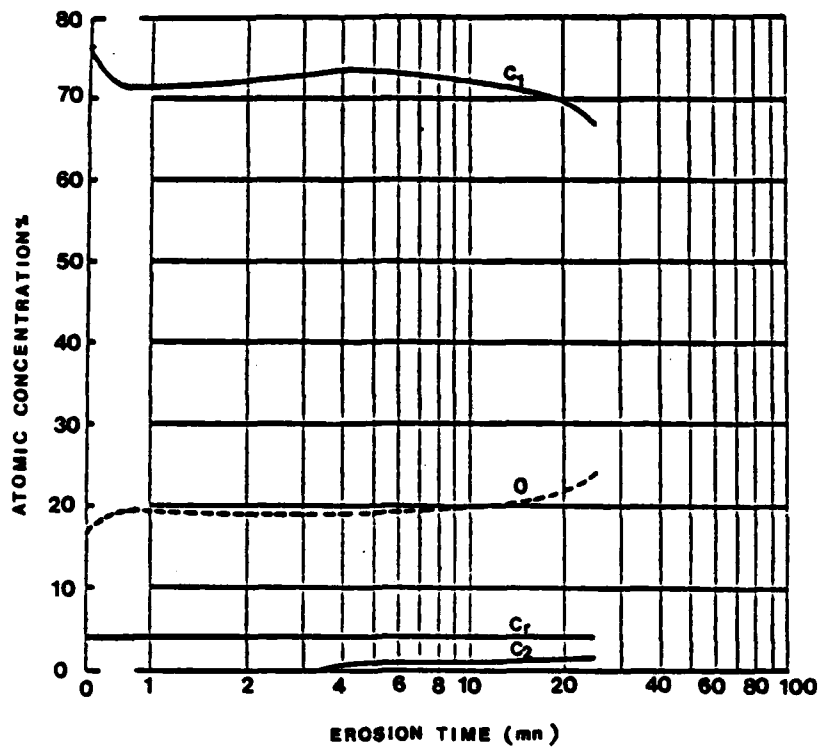figure 13 : As above. Non-glazed area

figure 14 : Curve of the atomic concentration of the elements of one point of
the surface, versus ionic erosion time : Cr_7C_3-NiCr after testing
in air at 900°C - glazed area

figure 15 : Same as above. Non-glazed area

3.2.1.3.4 : Fourth phase of friction : $T > T_{ox}$

Above T_{ox}, we observe the beginning of catastrophic oxidization of the coating. Even if the friction remains within acceptable limits, there is such an increase in wear that the coating is rapidly distroyed.

3.2.1.4 : The special case of friction in a vacuum :

The sliding friction behaviour of carbon based cermet coatings in a vacuum was briefly analysed at $1.3 \cdot 10^{-4}$ Pa (10^{-6} Torr) with sequential tests.

In the case of TiC-Ni, the coefficient of friction is abnormally low under 200°C, since it is 3 to 5 times lower than the coefficients of Ni on Ni and TiC on TiC friction, that can be found in publications [25, 26, 27, 28, 29] . This is probably due to the adsorbed films which are not damaged during short tests (3 mn) : an increase in pressure was observed, which was due to the desorption of adsorbed films.

Then, with the increase in temperature, the friction becomes bad. This is reminiscent of the friction behaviour of metals, and could show the influence of the binder. The following procedure pointed up this influence : we performed two tests, at 550°C and 700°C. In both cases, seizure appeared immediately. To make sure that Ni was responsible for such behaviour, we performed another test at 700°C. The Ni had been removed before testing from the surfaces of the samples, by dissolution in weakly diluted (10%) sulfuric acid doped with potassic chlorate (we obtained Ni/Ti = 0,11). In this way, we obtained a relatively low and regular coefficient of friction (fig. 16) during the whole test (90 mn). The wear rate was $3.1 \cdot 10^{-5}$ mm^3/Nm, which is high compared to tests in air. This rate may be due to the separation of carbide grains as a consequence of the removal of the binder. The most curious observation is related to the formation of glazed layers in a vacuum. As stated above, the formation of glazed layers on carbide coatings in air seems to be connected to the appearance of amorphous carbon in the friction interface. The analysis of the glazed layers in a vacuum did not point up any important differences from those obtained in air, except for the amounts of Nickel. More particularly, large quantities of amorphous carbon were detected on the

surfaces. This carbon could only come from oxidized carbides : we thus tried to find the source of the oxygen. Careful analysis of the records of our tests showed an increase in ambient pressure to $1.3 \cdot 10^{-3}$ Pa (10^{-5} mm Hg). We can suppose that the oxygen incorporated into the material during manufacturing, was freed thanks to the friction and vacuum.

      This study clarifies (i) the influence of the binder during friction and (ii) the influence of oxidization, which induces the disappearance of metallic type friction as well as the appearance of amorphous carbon in the interface, and thus favours the formation of glazed layers.
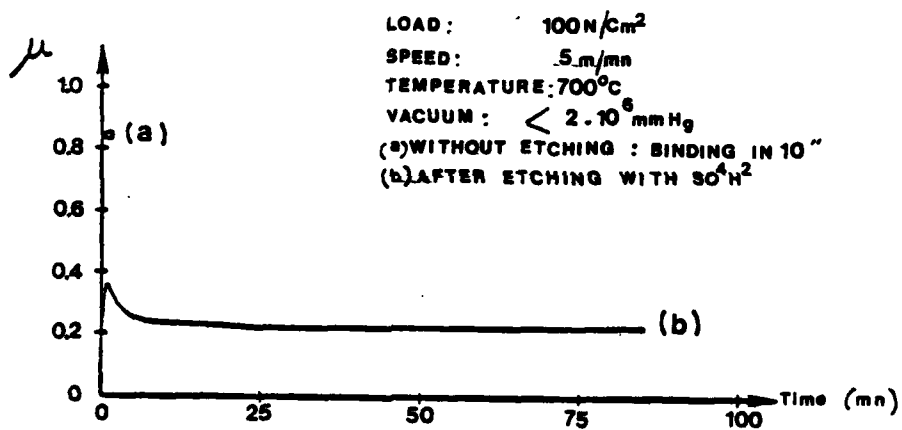

figure 16 : Effect of the Ni binder on the sliding friction of TiC-Ni, sliding against itself in a vacuum :

a) - ground surfaces

b) - surfaces with reduced Ni due to etching with SO_4H_2

3.2.2 : Friction of oxide-based ceramic coatings :

Oxides are a group of materials whose importance is increasing constantly. In the field of tribology, their importance is increased by the fact that the friction and wear of most industrial materials working at elevated temperatures in air are determined by the nature of the oxides that appear on their surfaces.

It is difficult to propose a single model for the friction behaviour of oxides like that of carbide based coatings. We will therefore discuss our results separately. They were obtained mainly through study of two simple oxides, easy to manufacture and of great industrial interest : chromium oxide (Cr_2O_3) and aluminium oxide (alumina : Al_2O_3).

3.2.2.1 : Friction tests :

3.2.2.1.1 : Cr_2O_3/Cr_2O_3

We carried out normal and sequential tests between 20 and 1000°C. Our results are shown in figures 17 to 20. In the first two figures, the temperature is the variable ; while in the two others, it is the load.
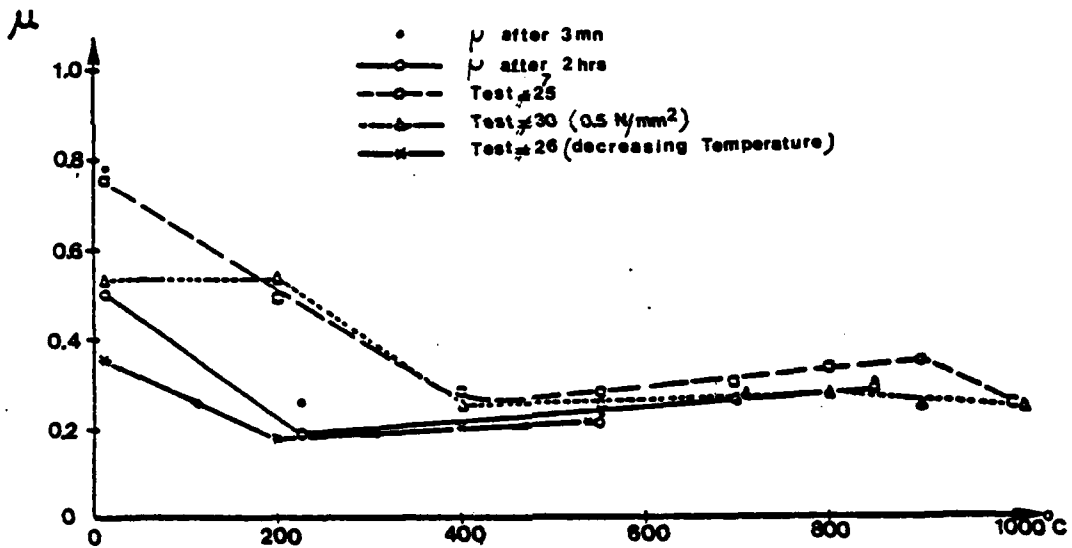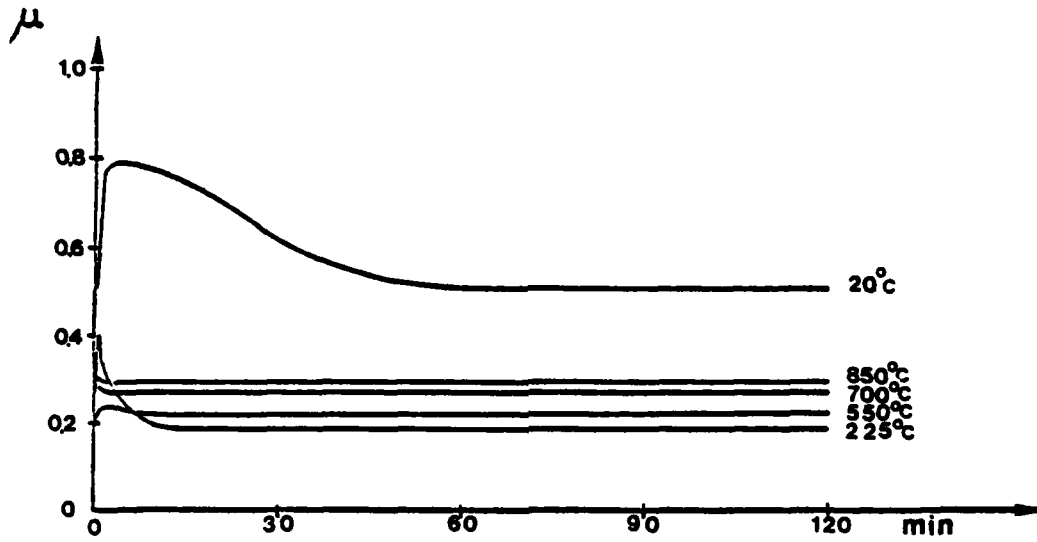
figure 17 : Variation of the coefficient of friction of Cr_2O_3 sliding against itself in air, versus time (1 N/mm^2, 5 m/mn)

figure 18 : Evolution of the coefficient of friction of Cr_2O_3 sliding against itself in air, versus temperature (1 N/mm^2, 5 m/mn)
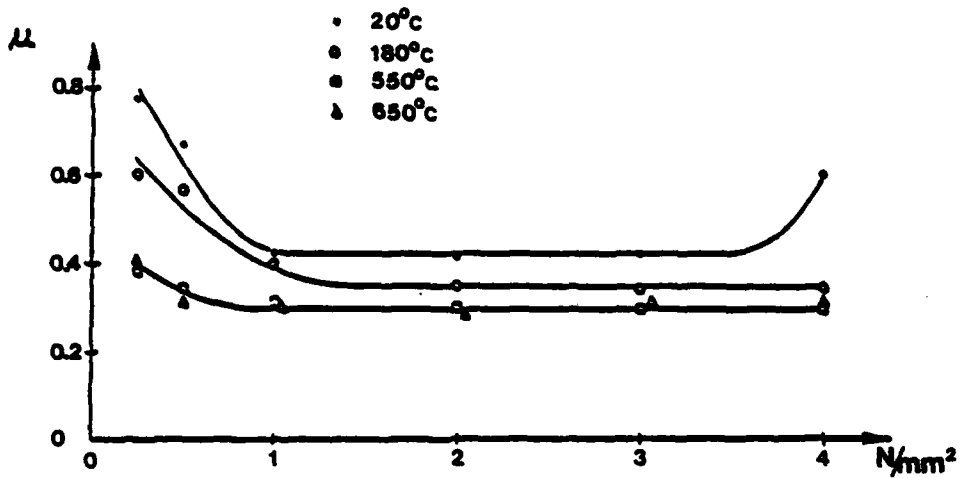
figure 19 : Evolution of the coefficient of friction of Cr_2O_3 sliding against itself in air, versus the apparent contact pressure (5 m/mn, 20 - 180 - 550 - 650°C)
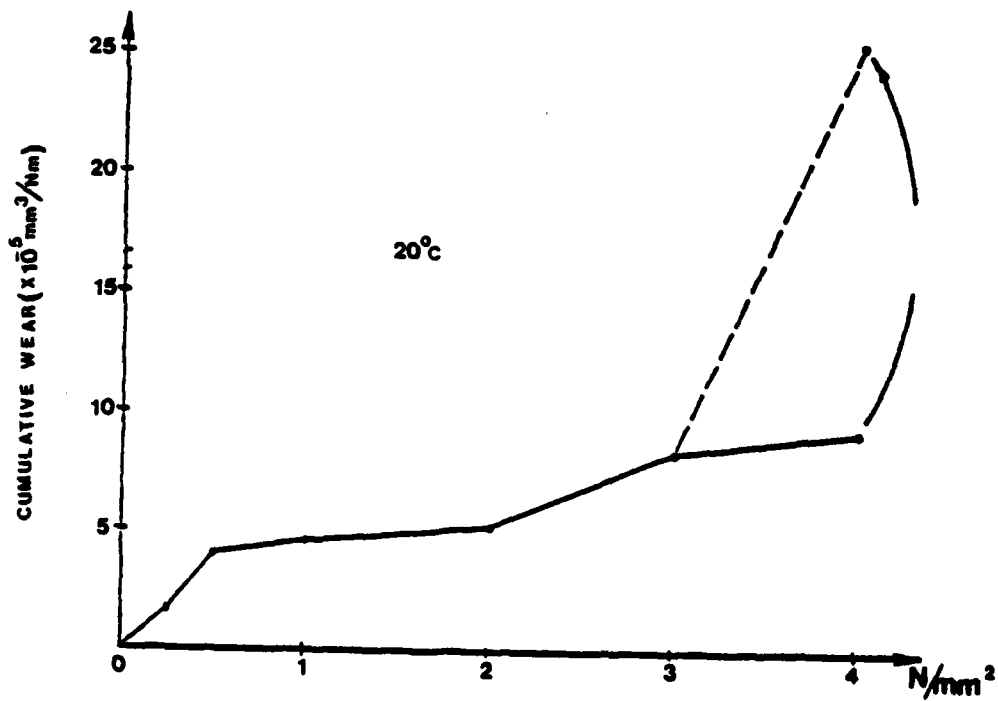
figure 20 : Cumulative wear measured after each grade of pressure. Test at 20°C illustrated in figure 19

3.2.2.1.2 : Al_2O_3/Al_2O_3

Only sequential tests were carried out with this material
(vs temperature or load). Our results are shown in figures 21 and 22.
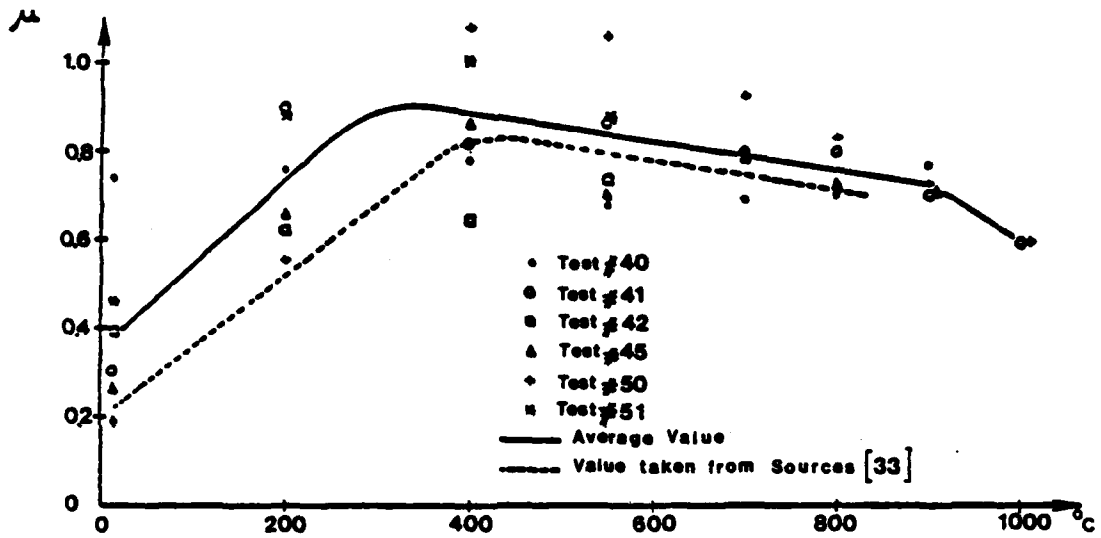
figure 21 : Evolution of the coefficient of friction of alumina sliding
in air against itself, versus temperature (1 N/mm^2, 5 m/mn)
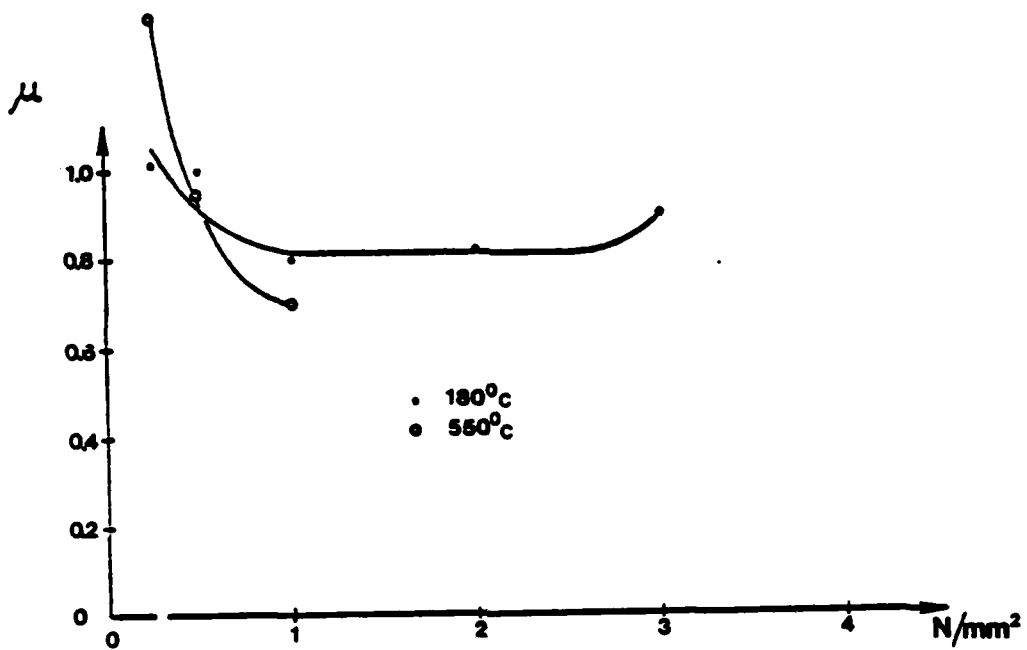
figure 22 : Evolution of the coefficient of friction of alumina sliding in air against itself, versus apparent contact pressure (5 m/mn, 180 and 550°C)

figure 22 bis: Evolution of the coefficient of friction of alumina sliding against chromium oxide in air, versus temperature (5 m/mn)

3.2.2.1.3 : Al_2O_3/Cr_2O_3

In this case, sequential tests were carried out and confirmed by normal tests. The results are given in figures 23, 24. (vs temperature or load).
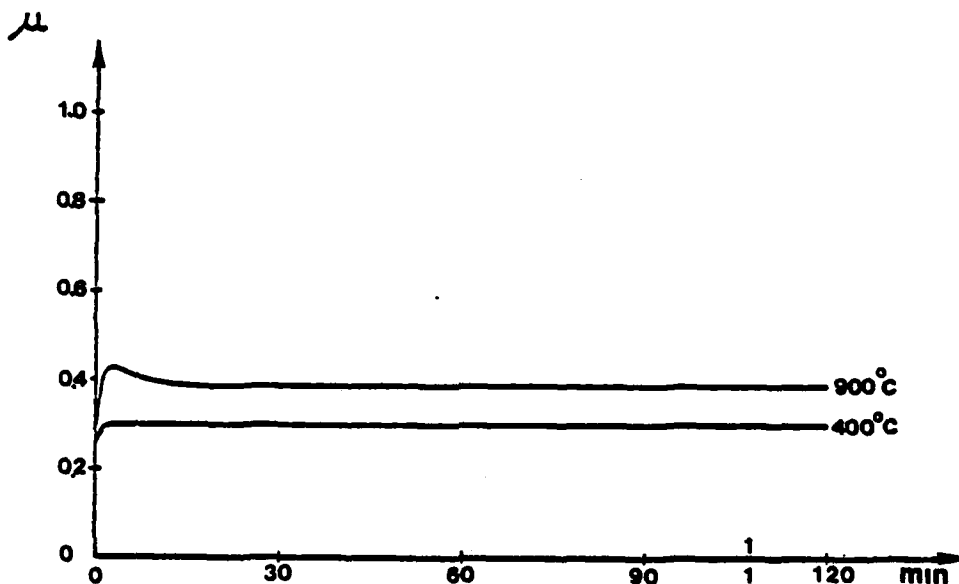
figure 23 : Variation of the coefficient of friction of alumina sliding against chromium oxide in air, versus time (1 N/mm^2, 5 m/mn, 400 and 900°C)

figure 24 : Evolution of the coefficient of friction of alumina sliding against chromium oxide, in air, versus apparent contact pressure (5 m/mn, 180 and 550°C)

3.2.2.1.4 : Special compounds :

Coatings of the following type :

$$x.Cr_2O_3 + (1 - x) Al_2O_3 \quad (0 \leqslant x \leqslant 1)$$

were tested against themselves, Al_2O_3 or Cr_2O_3. The results are given in figures 25 to 27.
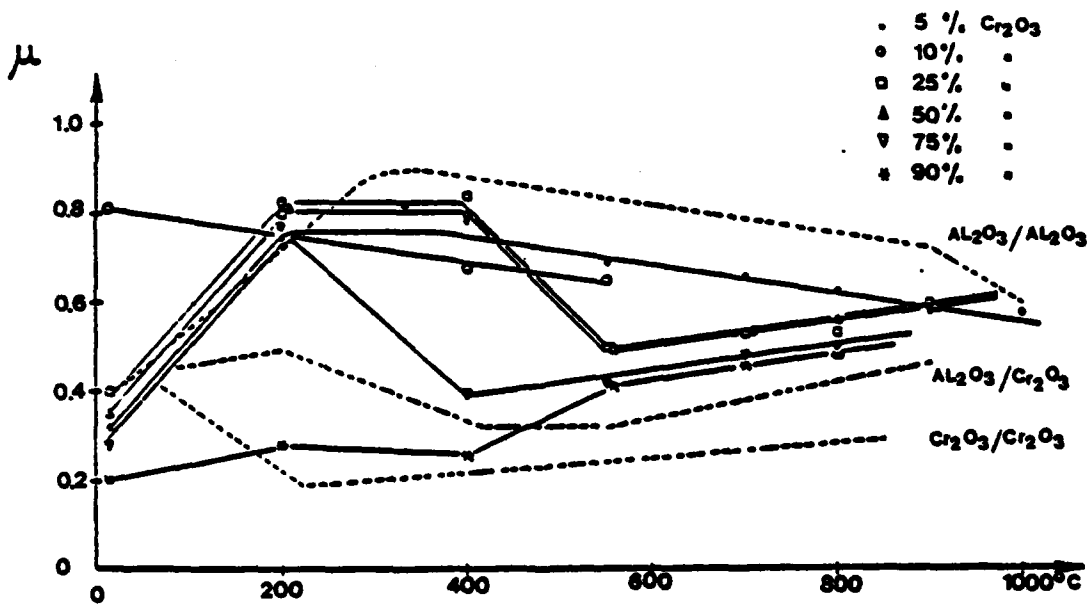
figure 25 : Evolution of the coefficient of friction of chromium
oxide-alumina compounds sliding against each other in
air, versus temperature (1 N/mm^2, 5 m/mn)

figure 26 : Evolution of the coefficient of friction of alumina sliding
against chromium oxide-alumina compounds in air, versus
temperature (1 N/mm^2, 5 m/mn)
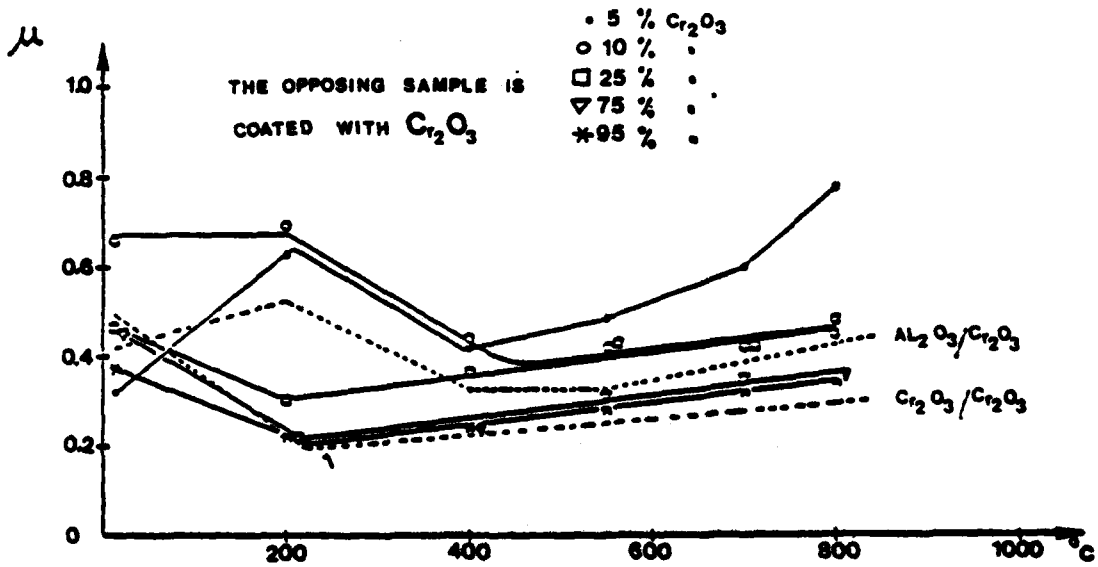
figure 27 : Evolution of the coefficient of friction of chromium oxide
sliding against chromium oxide-alumina compounds in air,
versus temperature (1 N/mm^2, 5 m/mn)

3.2.2.1.5 : Tests in a vacuum :

The pressure was lowered down to 2.6×10^{-4} Pa $(2.10^{-6}$ Torr). The results concerning these tests are given in figures 28 to 30. We have tested :

- Cr_2O_3/Cr_2O_3

- Al_2O_3/Al_2O_3

- Al_2O_3/Cr_2O_3
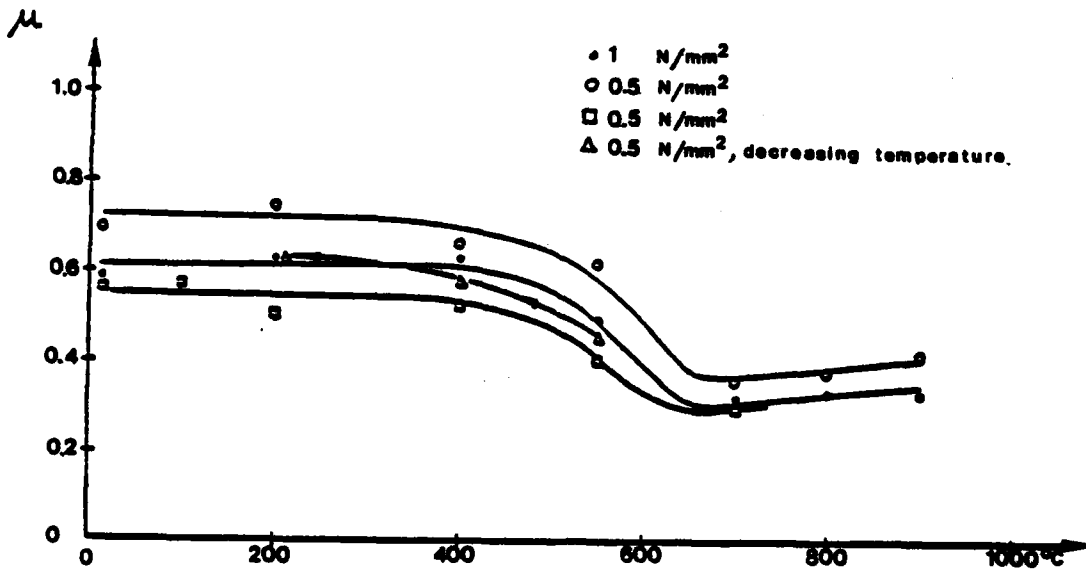
figure 28 : Evolution of the coefficient of friction of chromium oxide
sliding against itself in a vacuum, versus temperature.
(5 m/mn)
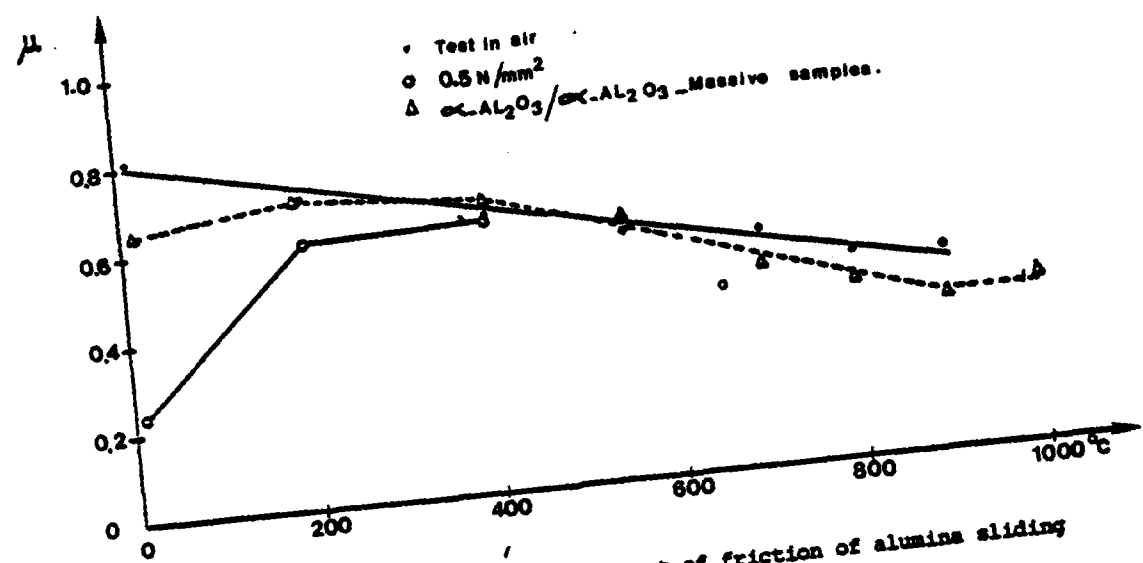
figure 29 : Evolution of the coefficient of friction of alumina sliding
against itself in a vacuum, versus temperature.
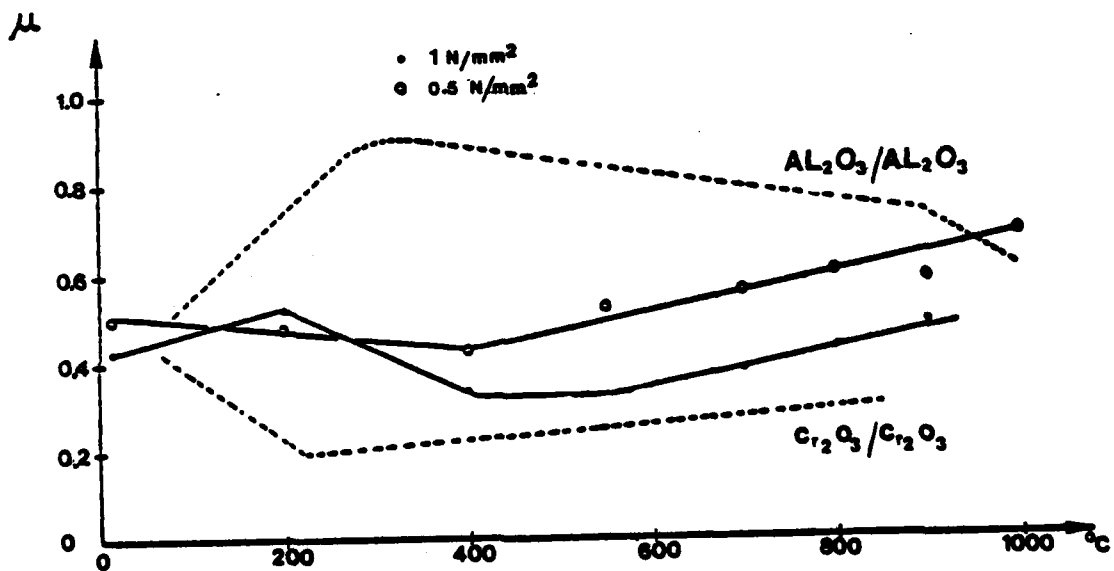(1 N/mm^2, 5 m/mn)
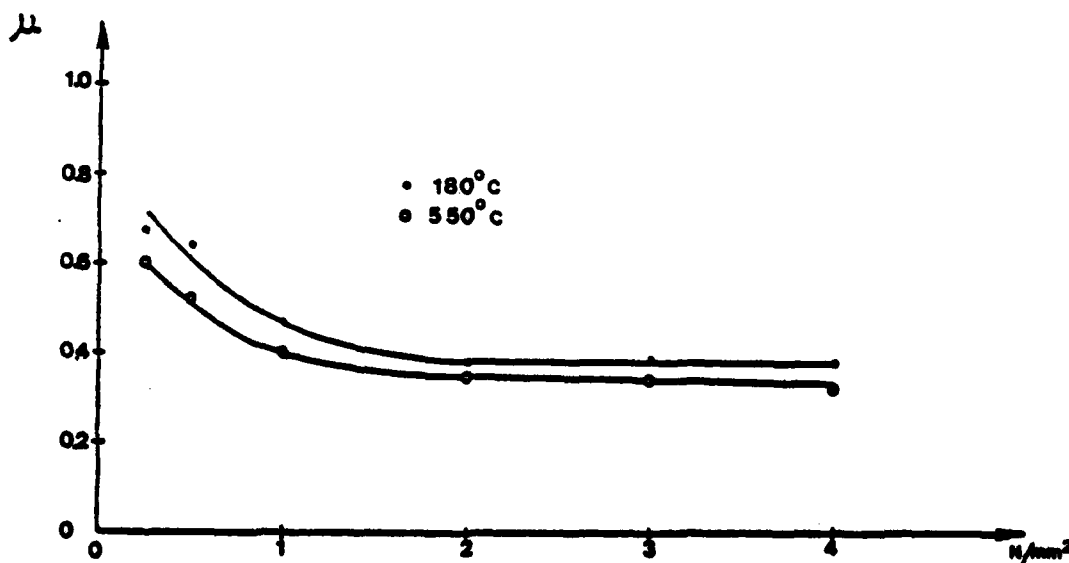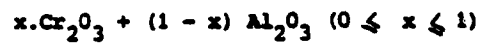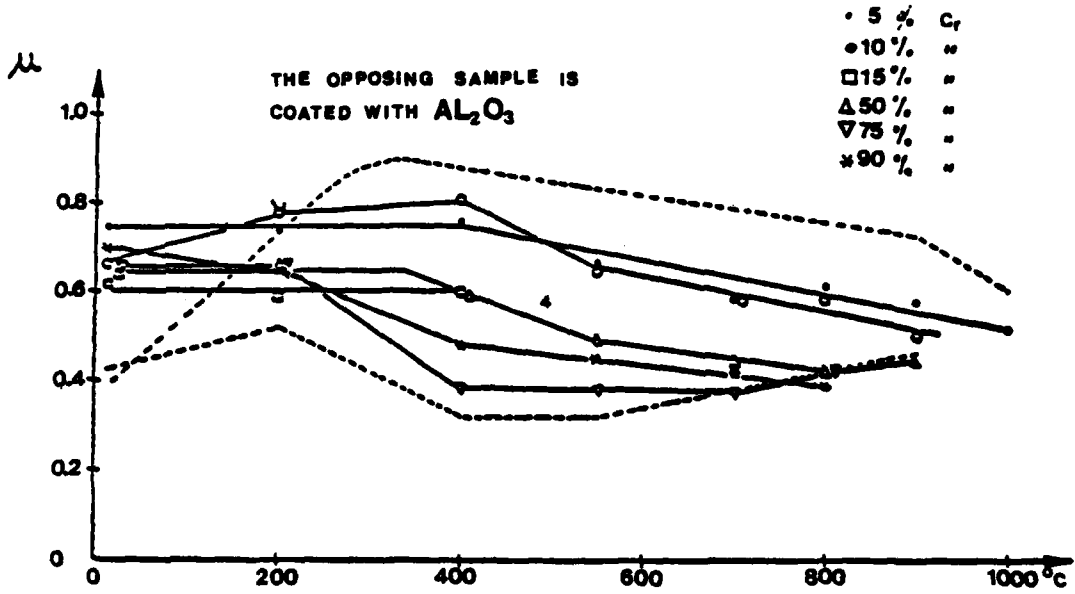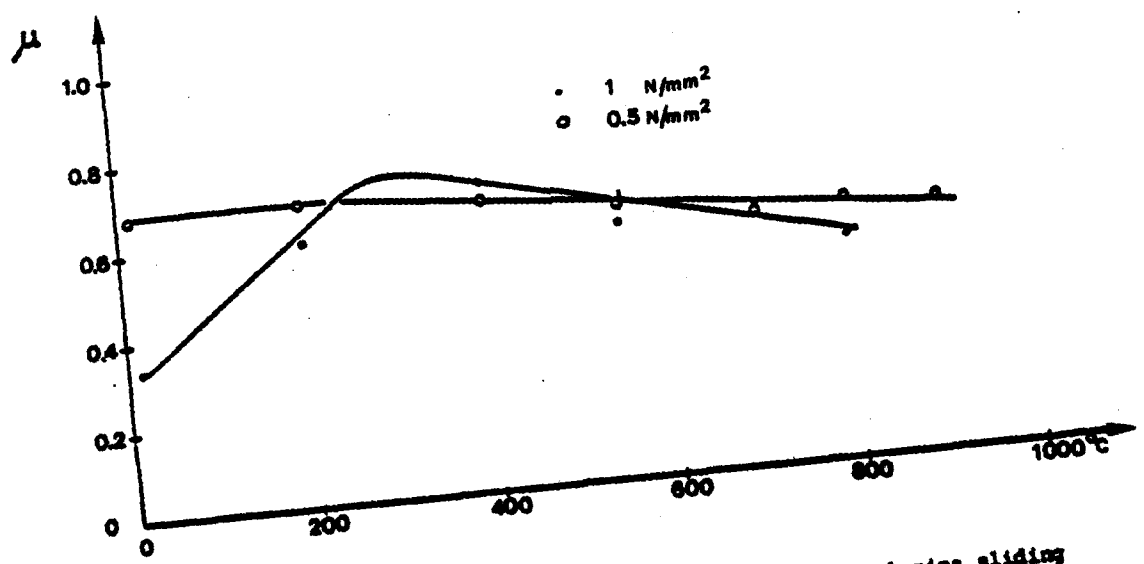

figure 30 : Evolution of the coefficient of friction of alumina sliding
against chromium oxide in a vacuum, versus temperature (5 m/mn)

3.2.2.2 : Analyses :

As shown before, and contrary to what was observed with carbide based coatings, it was not possible to discover a general behaviour for the oxide based coatings. We will thus discuss the results of our analysis for each of the tested couples. These couples are the following :

- Cr_2O_3/Cr_2O_3

- Al_2O_3/Al_2O_3

- Al_2O_3/Cr_2O_3

- Special compounds $xCr_2O_3 + (1 - x) Al_2O_3$ $(0 < x < 1)$

3.2.2.2.1 : Cr_2O_3/Cr_2O_3

X-Ray analysis of the surfaces did not permit detection of any other material than Cr_2O_3.

The evolution of the roughness parameters (Ra and R_T) versus temperature (with normal type tests, from 20°C up to 850°C) is given in table 6. Glazed surfaces were always obtained, except in the test at room temperature (20°C). Above 550°C, we observed the appearance of cracks on the edges of the samples. This phenomenon increased with the temperature, but never reached the sliding surfaces.

Microhardness measurements were done on the surfaces after normal tests. The results are listed in figure 31. The value shown is the average of at least 12 measurements made by two different operators. We can observe that the hardness of the material increases with the testing temperature. In addition, we noticed that the film that forms on the surfaces evolves in an interesting way : it begins as a powder at low temperature, and becomes increasingly compact and cohesive as the temperature increases.

H_v

4000

2000

Cr_2O_3 / Cr_2O_3

———— After 2 hrs at 20°C
———o———— After 2 hrs at 225°C
———•———— After 2 hrs at 550°C
———•———— After 2 hrs at 700° and 850°C

1000

400

$n=1.73$
$n=1.69$
$n=1.72$
$n=1.62$

200

100
80

60

40

$n=1.62$ $n=2.18$
$n=2.0$ $n=1.99$

20

10

H_v LOAD (g)	After 2 hrs at 20°C	After 2 hrs at 225°C	After 2 hrs at 550°C	After 2 hrs at 700 and 850°C
15	1915 (3.8)	2283 (3.5)	—	—
25	1954 (4.9)	2289 (4.5)	3047 (3.9)	3209 (3.8)
50	2128 (6.6)	2263 (6.4)	2575 (6)	3180 (5.4)
100	1854 (10)	1970 (9.7)	2190 (9.2)	3209 (7.6)
200	1670 (14.8)	1740 (14.6)	2228 (12.6)	2803 (11.5)
300	1574 (18.6)	1625 (18.5)	2093 (16.5)	2472 (15)

H_v in daN/mm²
(—) average value of the diagonal in μm

2
1   2   4   6 8 10   20   40   60 80 100 diagonale (μm)

figure 31 : Measures of microhardness in Cr_2O_3 coatings. Above,
Log HV = f(Log d) ; below, Log W = f(Log d)
(HV = microhardness, d = diagonal, W = load, n = slope)

Testing Temperature (°C)	Before test	20	225	550	700	850
Ra (m)	0,123	0,176	0,052	0,026	0,029	0,027
Rt (m)	1,664	2,483	0,892	0,809	0,693	0,775

Table 6 : Roughness parameters Ra and Rt of the surfaces of Cr_2O_3
after tests at 20, 225, 550, 700 and 850°C.

Temperature	400°C	900°C
ratio Cr/Al on Al_2O_3	0,0345	0,0547
ratio Al/Cr on Cr_2O_3	0,0447	0,0454

Table 7 : Cr/Al and Al/Cr ratios measured respectively on Al_2O_3 and Cr_2O_3
after continuous type tests at 400 and 900°C.

Roughness	Al_2O_3		Cr_2O_3	
Temperature	Ra	Rt	Ra	Rt
400°C	0,104	2,008	0,051	1,228
900°C	0,088	1,532	0,071	1,268

Table 8 : Variation of the roughness parameters Ra and Rt of Al_2O_3 and
Cr_2O_3, versus test temperature.

3.2.2.2.2 : Al_2O_3/Al_2O_3

After testing, the Al_2O_3 coatings are very damaged. Cracking of the edges is observed systematically above 550°C ; the coating-substrate interface is often sheared ; an abundant wear powder is obtained.

Optical and electronic microscopy show characteristic surfaces on which smooth and glazed areas can be seen. Their sizes vary from several tenths of a millimeter to several millimeters. These areas, which are quite numerous, are distributed on the whole sliding surface and surrounded by much wear debris.

X-ray diffractometry of the surfaces shows no evolution of the phases of alumina below 900°C. In air above 900°C, an incomplete transformation $\gamma \rightarrow \delta$ can be observed. In a vacuum, we observed a total transformation of alumina in $\alpha - Al_2O_3$: these different behaviours in air and in a vacuum have not been explained until now.

3.2.2.2.3 : Al_2O_3/Cr_2O_3

On a macroscopic scale, there is no noticeable morphologic difference between Al_2O_3 and Cr_2O_3.

Table 7 gives the results of microscan measurements : we observe that there is reciprocal transfer of both materials.

Table 8 gives roughness parameters Ra and Rt versus test temperature : these results show that the increase of temperature increases the roughness of alumina, and decreases that of Cr_2O_3.

Microhardness measurements were only carried out on the alumina sample, for it is easy to locate the layer with the optical device of the microhardness test apparatus : we can observe that the superficial hardness of the samples increases with test temperature.

This is probably related to the evolution of the chromium ratio on the surface of the Al_2O_3 sample : this ratio increases with temperature too.

3.2.2.2.4 : Special compounds :

Three types of tests were carried out with these materials, in
air :
- the special compound against itself
- the special compound against Al_2O_3
- the special compound against Cr_2O_3

X-Ray analyses did not permit detection of the formation of new
compounds. However, such compounds must exist because it is possible to
observe surface layers of different colors (from light pink to dark green).
This color variation is reminiscent of that of the solid solutions
Al_2O_3-Cr_2O_3.

Microanalysis of alumina-based surfaces clearly showed the presence
of Cr, which was not present before testing. Its ratio increases with the
Cr_2O_3 rate of the opposing sample.

3.2.2.3 : Discussion :

The curves show that two phases can be distinguished in this
friction :

- a transient phase : the lower the temperature, the more pronounced it is.
- a stable phase where the coefficient of friction depends on the temperature.

Our work deals especially with the second phase, although the first
is important. The evolution of the coefficient of friction depends on the
pairing of the materials : therefore, we will discuss our study pair by pair.

3.2.2.3.1 : Cr_2O_3/Cr_2O_3

The evolution of the coefficient of friction, as well as the wear of
this pair, suggest the existence of two phases of this friction (fig. 17 to 20) :

- under 200°C : friction is high and of poor quality
- from 200°C to 900°C : friction is low and regular and wear is negligible.

During the first phase, the environment seems to have little
influence on friction : if it is 0.5 in air, it is 0.6 in a vacuum. After
the test there was practically no wear of the sliding surfaces, which,
however, had a powdery appearance with a few thin scratches. These miniscule
particles adhere physically to the surfaces allowing the particles to
circulate in the sliding interface in an almost closed circuit. This phenomenon
results in the formation of a film of compacted debris at the end of the
transient phase. The film increased the real contact area and thus decreased
the real contact pressure, and also slowed down the process of creating wear
particles. In this phase we also varied the load, between 0.25 and 4.5 N/mm^2
(see figures). We observed a high coefficient of friction for pressures below
1 N/mm^2 as well as for pressures above 3 N/mm^2. In addition we can note that the
rate of wear is higher with lower loads than with higher loads. However, after
cleaning the samples in an ultra-sonic tank the loss of mass became very
significant, which shows that most of the debris remain at the interface and
adhere slightly.

During the second phase of sliding (between 200°C and 800°C) we
observed a change in the behaviour of the sliding pair, since the coefficient
of friction became low and regular, and wear negligible. It is during this
second phase that glazed frictional surfaces appeared. Under these conditions,
wear is comparable to that of the best performances of anti-wear treatments,
and the roughness parameters show that the obtained roughness is comparable
to that after the best polishing. Finally, the microhardness measurements
indicate that the compactness of the surface films increases with temperature.

We should note that above 550°C thermal cracks appear, resulting
in spalling at the edges of the samples. The finishing scratches often serve
to begin the cracks.

The negligible wear and the absence of debris suggest that glazing
is not due to a process of formation and compaction of particles followed by
a plastic deformation (as in alumina). The formation of glazed layers on
Cr_2O_3 begins at relatively low temperatures (200°C) and occurs rapidly as
shown by the short transition phase of the friction coefficient. Under these
conditions, the wear induced by sliding is negligible, and scratches from
lapping are still visible. These layers have the appearance of a very smooth
shiny surface with a beautiful mirror effect.

The refractarity of the material and the surface morphology of the layer analysed by scanning microscope indicated that thermal softening and plastic deformation are not responsible for this layer.

To explain the constitution of this glazed layer, we proposed a new explanation for the absence of wear debris and the rapidity of formation of the glazed film : the development of a very thin and shiny layer on the sliding surfaces of chromium oxide/chromium oxide friction in oxidizing atmosphere, occurs because of the heat engendered by the friction at the level of the asperities which oxide according to the reaction :

$$Cr_2O_3 + \frac{3}{2} O_2 \qquad 2 \, Cr \, O_3$$
$$\text{(s)} \qquad \text{(g)} \qquad \qquad \text{(g)}$$
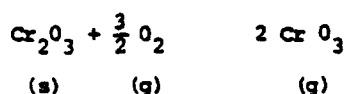
. This gives a smooth erosion of the tips of the asperities without creation of debris. The gas produced ($Cr \, O_3$) can be released into the atmosphere or even condensed in the colder zones, such as the hollows between asperities where it is again transformed into Cr_2O_3, which implies considerable difficulty in demonstrating the presence of $Cr \, O_3$. In support of this hypothesis, we will cite various bibliographic sources : the weight loss of Cr_2O_3 in oxidizing atmosphere above 1000°C was well established by ref. [30]. The reaction cited above has been used by many teams [30, 31, 32].

Finally, this process may explain the transfer of chromium oxide on alumina during the friction of Cr_2O_3/Al_2O_3.

The friction tests in a vacuum also tend to confirm our hypothesis. The morphology of the obtained surfaces shows a network of cracks and smooth areas (due to the release of gas), juxtaposed with abrasive-type damage with decohesion and fracturing of oxide particles.

3.2.2.3.2 : Al_2O_3/Al_2O_3

The results of the tests are shown in fig. 21 and 22, where each point represents the mean value of the friction coefficient after 3 mn. The sliding is very jerky (stick-slips) and the friction, between 20 and 550°C, is catastrophic with maximal values reaching 1.8 $\pm$ 0.5.

When the temperature increases, the friction coefficient quickly rises to a maximum at about 400°C, then it decreases. We can distinguish two phases in the friction :

- under 400°C
- above 400°C

In the first phase, the increase of the friction coefficient was attributed to the progressive desorption of water vapor, which, at ambient temperature, plays a very important protective rôle. The jerky sliding is caused by abrasive processes at the frictional interface. Similarly, plastic deformations contribute significantly to the dissipation of the frictional energy and to the appearance of intergranular cracks. We have severe wear giving large quantities of debris in a very fine powder.

In the second phase, the behaviour of alumina changes. We have a reduction of the friction coefficient with the increase of the temperature, while the influence of the water vapor is completely eliminated. This reduction can be attributed to the significant decrease in the thermal conductibility of alumina between 400 and 900°C. The evacuation of the heat is braked. The difference in temperature between the contacting zones and the coating is sufficient to facilitate shearing through thermal softening of the surfaces : the friction coefficient decreases. Then superficial films are formed through agglomeration and compacting of wear debris. These films are thermally softened, as demonstrated by the presence of scratches. These are not really continuous films, but rather series of glazed areas of variable size. Their dimensions increase with the temperature and the velocity. The formation mechanism of these glazed films would be the following :

- emission of very small wear debris
- agglomeration and compacting of these debris
- high plastic deformation

The tests in a vacuum showed that the atmosphere did not play an important rôle in the friction of alumina : the variation of the friction coefficient is very similar to that found in air.

3.2.2.3.3 : Al_2O_3/Cr_2O_3

The test results are shown in fig. 22 b and 23. We can see that the evolution of the friction coefficient is situated between that of the pairs Al_2O_3/Al_2O_3 and Cr_2O_3/Cr_2O_3. We have again two phases : one below 400°C and another above.

We studied in particular the second phase which is more pertinent for high temperature applications.

In this phase the friction coefficient increases in a linear relationship to the temperature. We can notice that we are near the behaviour of the pair Cr_2O_3/Cr_2O_3. This is due to the significant transfer of Cr_2O_3 into the Al_2O_3. We can also see some Al_2O_3 on the Cr_2O_3. In the first case this transfer is due to the same mechanism that we suggested for the glazing of Cr_2O_3 : formation of gaseous $Cr\ O_3$ which condenses on the colder areas. It is the only mechanism that explains satisfactorily the transfer without emission of debris. In the second case, we think that the wear debris from the first second of sliding are trapped. This hypothesis is supported by the fact that, if the quantity of Cr_2O_3 on Al_2O_3 can reach significant proportions, the amount of Al_2O_3 on Cr_2O_3 always remains the same.

In a vacuum (see fig. 30) the friction characteristics are close to those of Al_2O_3/Al_2O_3, because of the absence of oxidation and because Al_2O_3 shears more easily than Cr_2O_3. The paucity of observations in this area, however, suggests we make these deductions with caution.

3.2.2.3.4 : Coatings with variable content :

Our observations (see fig. 25 to 27) show that :

- the addition of a few percentage points of Cr_2O_3 to alumina markedly improves the coefficient of friction of Al_2O_3/Al_2O_3 pairs, without noticeable variation in their thermal stress resistance.

- the addition of Cr_2O_3 in larger amounts ($> 10\%$) improves the friction coefficient even more, but the cohesion among the coating particles is reduced, which results in an increase in the wear rate.

- the addition of a few percentage points of Al_2O_3 to the Cr_2O_3
coatings barely changes the friction coefficient of the Cr_2O_3/Cr_2O_3 pairs.

Generaly speaking, we can say that the presence of Cr_2O_3, governs
the sliding friction of these oxide combinations. This is especially true
above a certain temperature, which is lower, the more the amount of Cr_2O_3
is high. These observations support our hypothesis concerning the transfer
mechanism of Cr_2O_3 in gaseous state.

CONCLUSIONS

We studied the evolution of the coefficient of friction between 20°
and 1000°C as a function of the temperature of various types of refractory
coatings. So we were able to show the existence of several mechanisms :

- At low temperature ($\theta < 400°C$)

The variations of the friction coefficient and wear were correlated
to the changes in the behaviour of superficial layers induced by adsorption -
desorption phenomena.

- At high temperature ($\theta > 400°C$)

We demonstrated the importance of oxidation in every case.

- Carbide based coatings

When the oxidation is low ($400 < \theta < 800$ to $1000°C$) the conditions
are present for the constitution of a glazed layer which induces low and
regular friction as well as negligible wear.

Increase in temperature leads to catastrophic wear which quickly
destroys the coating.

The glazed layers are composed of a mixture of large amounts of
oxides and amorphous carbon. The carbide particles act as reservoirs of
carbon, released by oxidation.

- Ceramic coatings

The chromium oxide contributes significantly to the glazing of
surfaces, which gives smooth and regular friction, as well as negligible
wear.

This glaze is a result of the oxidation of chromium oxide which
is transformed into gaseous $Cr\,O_3$, which then condenses in the cold zones
and is retransformed into Cr_2O_3.

With alumina/alumina friction, the constitution of little glazed
areas of compacted debris eliminates the abrasive nature of the wear,

improving friction and reducing wear.

With Al_2O_3-Cr_2O_3 combinations, we demonstrated that the Cr_2O_3 determines the process of friction and wear, even in small amounts.

Finally, we should note that, in the range of the temperatures studied, the carbide based cermet coatings have a much higher thermal stress resistance than oxide based ceramic coatings.

SELECTED BIBLIOGRAPHY

1 - BOWDEN F.P. and TABOR D. : The Friction and Lubrication of Solids
Clarendon Press, 1958, Books I and II.

2 - GREME H. and KOLASKA J. : Hard materials as the basis for wear resistance
Metallurgical Aspects of Wear, 319-352
Deutsche Gesellschaft für Metalkunde E.V., 1981.

3 - PETERSON M.B., FLOREK J.J. and LEE R.E. : Sliding characteristics of metal
at high temperatures,
ASLE Transac, 1960, 101-109.

4 - RABINOWICZ E. : Influence of surface energy on friction and wear phenomena,
J. Appl. Physics 32, 8, 1961.

5 - ZEMAN K.P. and COFFIN L.F. : Friction and wear of refractory compounds
ASLE Transac, 3, 1960, 191-202.

6 - BUCKLEY D.H. : Adhesion of metals to a clean iron surface studied with
L.E.E.D. and Auger electron spectroscopy,
Wear, 20, 1972, 89-103.

7 - SEMENOV and POZDNYAKOF : Structures and Properties of Heat Resistant Metals
and Alloys,
Pridantsev A. Sc. URSS, Trad. ISRAEL 1970,
Keter Press Jerusalem.

8 - MOLGAARD J. : A discussion of oxidation, oxide thickness and oxide transfer
in wear,
Wear, 40, 1976, 277-291.

9 - HAMILTON G.M. and GOODMAN L.E. : The stress field created by a circular
sliding contact,
J. Appl. Mech., June 1966, 371-376.

10 - SUH N.P. : An overview of the delamination theory of wear,
WEAR 44, 1977, 1-6.

11 - SUH N.P. : The delamination theory of wear,
WEAR 25, 1973, 111-124.

12 - JAEGER J.C. : Moving sources of heat and the temperature of sliding contact,
Proc. R. Soc. N.S.W. 76, 1942, 203.

13 - HORNBOGEN E. : Microstructure and Wear,
Metallurgical Aspects of wear, p 23-49,
Deutsch Gesellschaft für Metallkunde E.V. 1981.

14 - CAMPBELL N.E. : Solid lubricants,
Standard handbook of lubrication Engineering, Mc GRAW-HILL.

15 - AYEL J. : Frottement et usure de métaux et composés réfractaires
Revue de l'institut français du Pétrole, L3, 11, 1968, 1413-1446.

16 - BUCKLEY D.H. and JOHNSON R.L. : The influence of silicon additions on friction
and wear of Nickel alloys at temperatures up
to 100° F,
ASLE Transac, 3, 1960, 93-100.

17 - PRANEVICIUS L. : Structure and properties of deposits grown by Jon-Beam
activated vacuum deposition techniques,
Thin Solid films 63, 1979, 77-85.

18 - FRELLER H. and HAESSLER H. : Deposition of tungsten-alumina composite films
                                  by oxide evaporation,
                                  Thin solid films 63, 1979, 377-382.

19 - BHARAT OHUSHAN : Development of R.F. sputtered chromium oxide coating for
                     wear application,
                     Thin solid films 64, 1979, 231-241.

20 - RIGNEY D.A. and GLAESER W.A. : The signifiance of near surface microstructure
                                   in the wear process,
                                   WEAR 46, 1978, 241-250.

21 - RIGNEY D.A. and HIRTH J.P. : Plastic deformation and sliding of metals,
                                 WEAR 53, 1979, 345-370.

22 - POMEY J. : Aperçu sur la plasticité adiabatique,
               Annals of the CIRP, XIII, 1966, 93-109.

23 - ZENER C. and HOLLOMON J.H. : Effect of strain rate upon plastic flow of steel,
                                 J. Appl. Phys. 15, 1944, 22-32, (cited by 1 and 22).

24 - REHBINDER P.A. and SCUKIN E.D. : Les phénomènes de surface dans la déformation
                                     et la fracture des solides,
                                     Séminaire de mécanique des surfaces,
                                     ISMCM, 17-19 Mai 1971.

25 - BROOKES C.A. : Bulk plastic flow and the frictional properties of titanium
                   carbide at high temperature,
                   WEAR 9, 1966, 103-117.

26 - MORDIKE B.L. : The frictional properties of carbides and borides at
                   high temperatures,
                   WEAR 3, 1960, 374-387.

27 - BARNES D.J. and POWELL B.D. : The friction and fragmentation of some
                                    refractory solids : the role of protective
                                    surface films,
                                    WEAR 32, 1975, 195-202.

28 - STOTT F.H., LIN D.S., WOOD G.C. and STEVENSON C.W. : The tribological behaviour
                                    of nickel and nickel-chromium
                                    alloys at temperatures from
                                    20 to 800°C,
                                    WEAR 36, 1976, 147-174.

29 - GRAS R. : Frottement à haute temperature du nickel,
          Mécanique, Matériaux, Electricité, 363, 1980, 87-99.

30 - CAPLAN D. and COHEN M. : The volatilization of chromium oxide,
                              J. Electromecanical Soc 108, 5, 1961, 458-442.

31 - GRAHAM H.C. and DAVIS H.H. : Oxidation/Vaporization kinetics of Cr_2O_3,
                              J. Amer. Ceram. Soc. 54, 2, 1971, 89-93.

32 - GRIMLEY R.T., BURNS R.P. and INGHRAM M.G. : Thermodynamics of the vaporization
                              of Cr_2O_3 : dissociation energies of
                              $Cr\ O$, $Cr\ O_2$, $Cr\ O_3$,
                              J. Chem. Phys. 32, 2, 1961, 664-667.

END

DATE
FILMED

'2 8